

A.I.F.A. - ITALIAN ASSOCIATION FOR FATIGUE IN AERONAUTICS  
DEPARTMENT OF CIVIL AND INDUSTRIAL ENGINEERING - UNIVERSITY OF PISA

Review of aeronautical fatigue investigations  
carried out in Italy  
during the period April 2019 - March 2021

by  
L. Lazzeri  
Department of Civil and Industrial Engineering  
University of Pisa - Italy

This document summarizes the principal research activities carried out in Italy about aeronautical fatigue in the period April 2019 – March 2021. The main topics covered are: operational load analysis, fatigue and fracture mechanics of metals, fatigue and damage tolerance of composites, Structural Health Monitoring, NDI methods.

ICAF Webinar, 30 June 2021

## CONTENTS

	Page
1. INTRODUCTION	7/1
2. MEASUREMENT AND ANALYSIS OF OPERATIONAL LOADS	7/1
2.1 - AM-X life monitoring (Leonardo Aircraft Division)	7/1
2.2 - Life monitoring of the TORNADO fleet (Leonardo Aircraft Division)	7/2
2.3 - EF Typhoon life monitoring (Leonardo Aircraft Division)	7/3
2.4 - Rotorcraft Usage Monitoring through Machine Learning Approaches (Leonardo Helicopter Division)	7/5
2.5 - C-27J program (Leonardo Aircraft Division)	7/7
3. METALS	7/8
3.1 - Fatigue behaviour of notched and unnotched materials	7/8
3.1.1 - Unique Materials for Advanced Aerospace Applications – UMA3 (Univ. Bologna)	7/8
3.1.2 - REACH regulation implementation (Leonardo Aircraft Division)	7/8
3.1.3 - One-up drilling process (Leonardo Aircraft Division)	7/9
3.1.4 - Fatigue analysis code (Leonardo Aircraft Division)	7/10
3.2 - Crack propagation and fracture mechanics	7/11
3.2.1 - Ti-6Al-4V Investment Casting HIP BSTOA Crack Propagation test data analysis (Leonardo Helicopter Division)	7/11
3.2.2 - Fatigue crack propagation of 3-D defects (Univ. Pisa)	7/11
3.3 – Corrosion and Fatigue	7/12
3.3.1 - Corrosion Effects Assessment on Fatigue Behaviour of Al 7475-T7351 (Leonardo Helicopter Division)	7/12
3.4 – Structural Health Monitoring of metallic structures	7/14
3.4.1 - Structural Health Monitoring – Acoustic Emissions (Univ. Bologna)	7/14
4. COMPOSITES AND FIBER METAL LAMINATES	7/15
4.1 - Investigation on Disbond Arrest Features in adhesive joints (Univ. Bologna)	7/15
4.2 - Effects of thermal residual stresses on the structural integrity of hybrid and composite elements (Milan Polytechnic)	7/17
4.3 - Structural Health Monitoring by means of Optical Fibres (Univ. Bologna)	7/20
4.4 - Obsolescence of Composite Materials of PSEs (Leonardo Helicopter Division)	7/21
5. NDI METHODS	7/22
5.1 - Probability of Detection for Visual Inspection (Leonardo Helicopter Division)	7/22
6. AIRCRAFT FATIGUE SUBSTANTIATION	7/24
6.1 - Damage tolerance of AW249 attack helicopter (Leonardo Helicopter Division)	7/24
6.2 - AW189 / AW139 / AW169 helicopter family (Leonardo Helicopter Division)	7/25
7. REFERENCES	7/26

## 1. INTRODUCTION

This paper summarises aeronautical fatigue investigations carried out in Italy during the period April 2019 to March 2021. The different contributions have been arranged according to the topics, which are operational load analysis, fatigue and fracture mechanics of metallic materials, fatigue and damage tolerance behaviour of composites, structural health monitoring and NDI methods. With respect to the last National Review, a paragraph dedicated to NDI methods has been inserted, on the basis of extension of ICAF interests towards structural integrity, in general. A list of references, related to the various items, is presented at the end of the document.

The review is based on the activities carried out within the various organisations belonging to A.I.F.A., the Italian Association for Fatigue in Aeronautics. The author gratefully acknowledges the fundamental contribution, which has made this review possible, given by several A.I.F.A. members, who are the representatives of Universities and Industries in A.I.F.A.

## 2. MEASUREMENT AND ANALYSIS OF OPERATIONAL LOADS

### 2.1 - AM-X life monitoring (Leonardo Aircraft Division)

On regular basis, every Italian National Review has given updated information on the rate of fatigue life consumption of the AM-X fleet, which is based on classic mechanical g-meter readings and on the basis of information about configurations and mission profiles. Up to now, more than 221 thousand flight hours have been monitored since the aircraft entered into service. As shown in fig. 1, the rate of growth of monitored hours is substantially the same of the flown hours, which means that all the airplanes (both strike and trainer) are monitored.

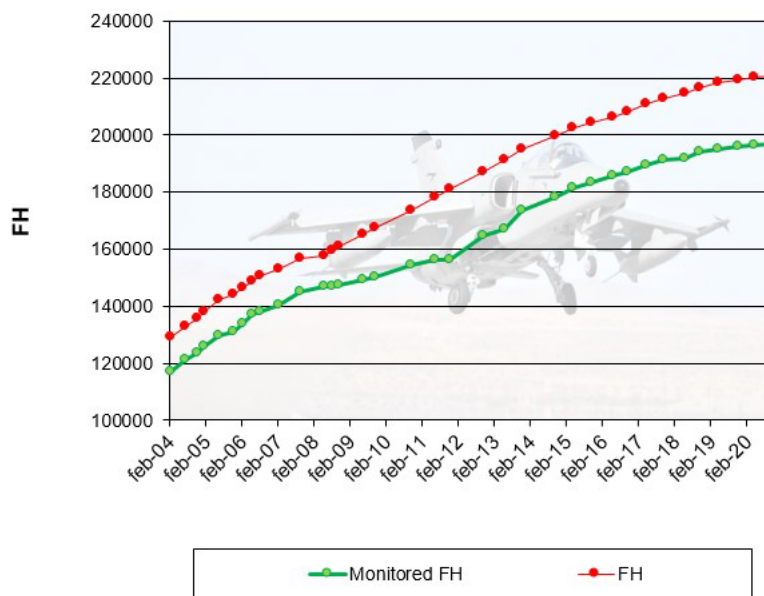


Fig. 1 – AM-X fleet monitored rates (FH): FH rate vs monitored FH rate are similar.

Leonardo Aircraft Division has defined a parameter for assessing the usage intensity of the various aircraft: this is the Load Severity Index (L.S.I.), defined as the ratio between the In-Service Life Damage and the Design Life Usage. In the last period of observation, a slight tendency towards lower severity utilisation rates (already present in the previous years) is confirmed, with an average value of 0.96 for the whole fleet, which anyhow means that the fatigue life consumption is substantially in line with design assumptions. The L.S.I. trend as a function of time (Fig. 2) shows a slight difference between the Strike aircraft (with a LSI index lower than 1) and the Trainer aircraft (which has on the contrary a LSI index higher than 1).

As an additional information, Fig. 3 shows the distribution of the L.S.I. index within the AM-X fleet: the usage severity is rather uniform, with the majority of the population in the range 0.7-0.9.

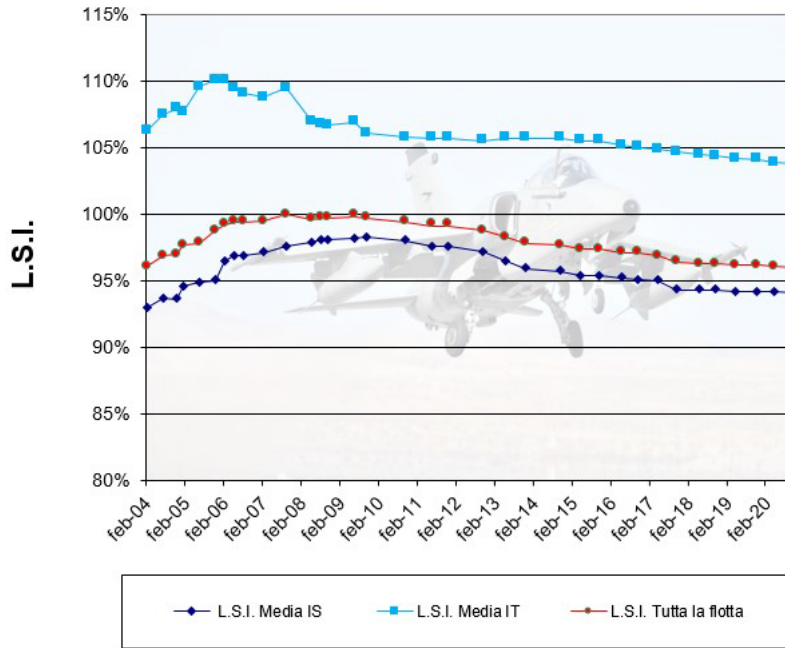


Fig. 2 – AM-X: Load Severity Index evolution with time.

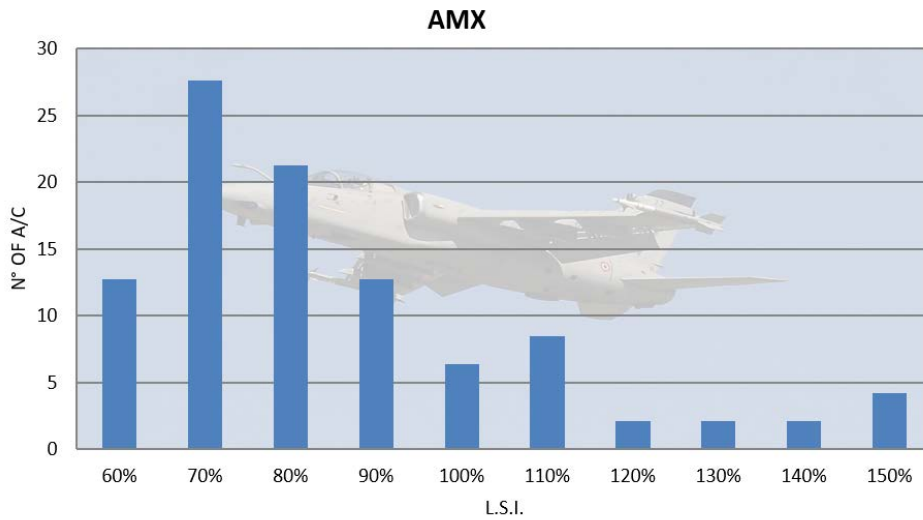


Fig. 3 - Distribution of the LSI within the AM-X fleet.

## 2.2 - Life monitoring of the TORNADO fleet (Leonardo Aircraft Division)

Tornado entered into service with the Italian Air Force in 1980 and, from the beginning of its activity to the end of 2016, about 300000 flight hours have been analysed by Leonardo Aircraft Division, on the basis of mechanical g-meter readings complemented by configuration/masses control.

In 2016, a new Monitoring System (Ma.Re.S – Maintenance Recorder System), based on more sophisticated calculation algorithms, entered into service. Currently, Leonardo is contracted only for problems concerning Ma.Re.S malfunctioning or updating of the database due to the implementation of the foreseen modifications that extend the life of specific airplane main components.

Up to now, no problem arose concerning the life consumption calculations. The only problem was related to the hardware, that did not read correctly some of the parameters used by the life consumption algorithms.

The aircraft service life has been extended recently from 4000 to 6000 Flight Hours and the individual tracking will be maintained in order to assure that a correct fleet management is performed and any possible anomalous fatigue consumption is identified.

### 2.3 - EF Typhoon life monitoring (Leonardo Aircraft Division)

Single Seater (SS) and Twin Seater (TS) versions of the EF Typhoon have been delivered to the Italian Air Force since the year 2003. The whole fleet is composed by more than 90 aircraft and up to now the fleet has been flying for more than 205000 Flight Hours, corresponding to about 80710 flights.

Individual Aircraft in-service monitoring is performed by means of the Structural Health Monitoring (SHM) system, an on-board parametric system. Some basic information about SHM has been provided in the previous editions of the National Review: ten significant locations are selected and monitored.

The Usage Factor is defined as the ratio between mean hourly consumption and the design one:  
(usage factor) = (in-service usage rate) / (design usage rate)

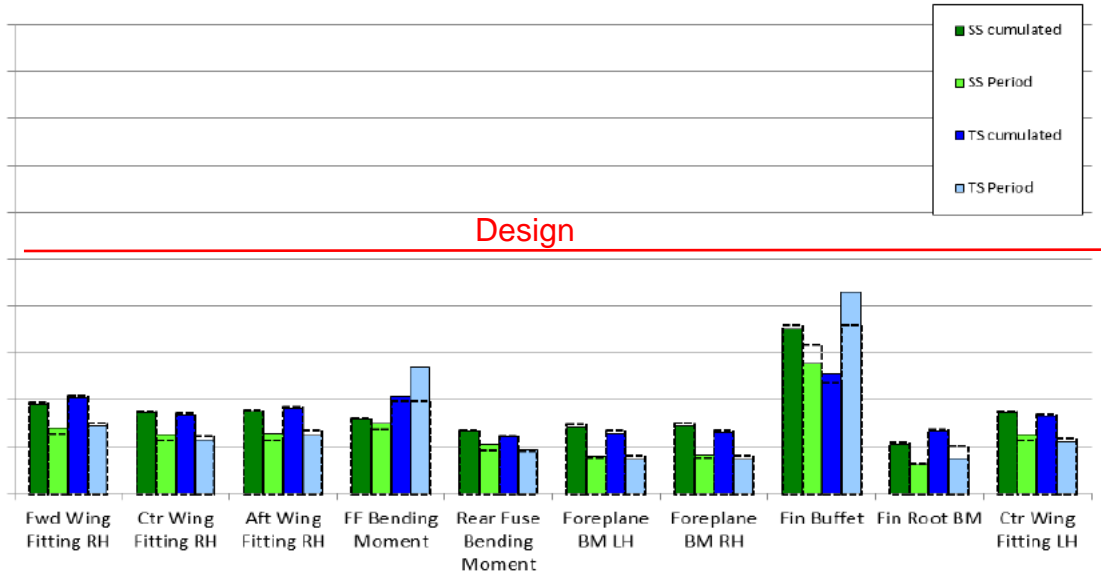


Fig. 4 – Usage Factor for the 10 monitored locations.

Figure 4 shows that the Usage Factor rate is below the design value for all the 10 locations. The trend is a decrease in all locations, as can be seen from the fact that the column relevant to the value in the period (typically 6 months) is often shorter than the one relevant to the cumulated average, i.e. the average value from the beginning of the monitoring. The lead location is number 8, for both SS and TS.

The Nz Spectrum is qualitatively reported in Fig. 5: both SS and TS fleets are flying within the design Nz envelope.

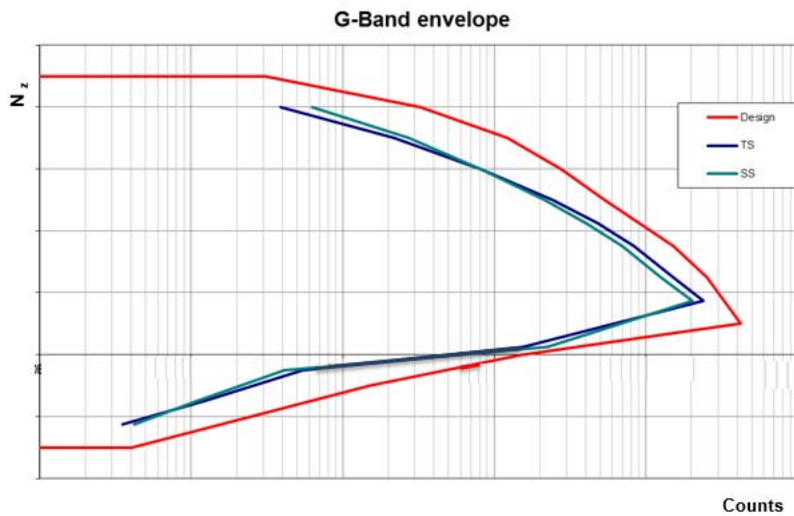


Fig. 5 – Non-dimensional Nz spectrum of the IAF Typhoon fleet.

The loads experienced during the phases of Wing Buffet occurrence are treated with a specific procedure, described in the following.

The Fatigue Life consumed at wing tip during the aircraft life is calculated by means of a method based on the use of four flight parameters: Angle of Attack, Equivalent Air Speed, Mach and Airbrake position, which are defined in the Flight Condition Duration Matrices (FCDM) retrieved from the Structural Health Monitoring System (an example is shown in Fig. 6). In particular, the method should identify the cells of the matrix which correspond to situations where the wing buffet occurs, as a consequence of the combination of the aerodynamic parameters. The Fatigue Life consumption is calculated through the multiplication of the FCDM matrix by the Dynamic Unit Damage Matrix (DUDM); each cell of such DUDM matrix contains the fatigue life consumption rate per unit of time elapsed.

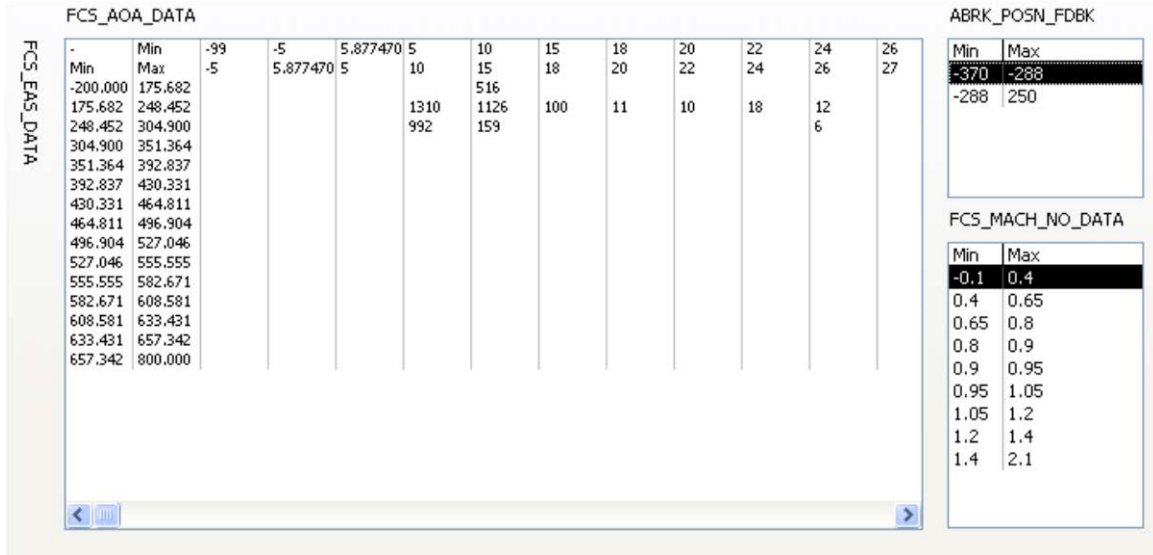


Fig. 6 - Example of Flight Condition Duration Matrix

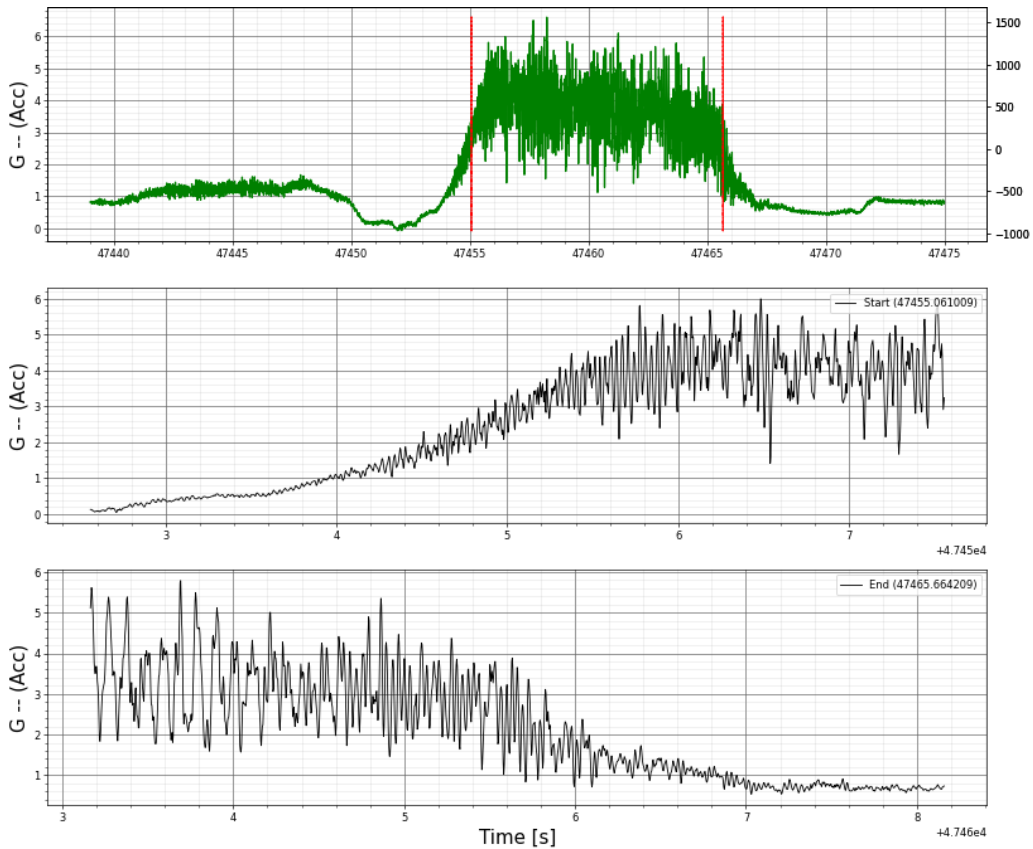


Fig. 7 - Examples of Time History recorded by the Accelerometer

The fundamental parameter for the fatigue damage calculation due to wing buffet is the assessment of the time that the aircraft spends in this condition; it is therefore important to study which are the aerodynamic conditions when buffet occurs. To support this activity, the recordings acquired by means of a dedicated aircraft, equipped with accelerometer and strain-gauge, have been analysed in order to develop a method able to define the occurrence of buffet conditions and to study the features of the phenomena during the flight. Figures 7 and 8 show examples of time histories, of the accelerometer and of the aerodynamic parameters.

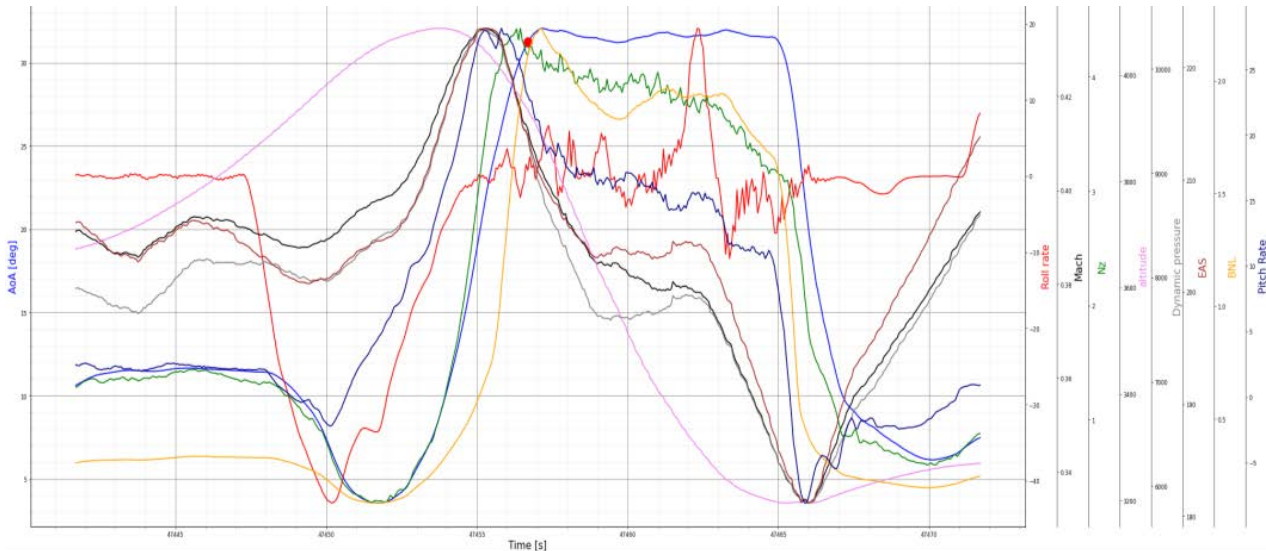


Fig. 8 - Example of Time Histories of Aerodynamic parameters.

#### 2.4 - Rotorcraft Usage Monitoring through Machine Learning Approaches (Leonardo Helicopter Division)

Flight Conditions Recognition (FCR) has provided the basis for the development of a Usage Monitoring System, installed by an increasing number of customers on their EH101 fleet. To satisfy the increasing number of requests for similar devices also on the helicopters of the 'Family' (i.e. AW169, AW139 and AW189), substantial improvements of the FCR methodologies have been studied, to allow an automatic and reliable analysis, in a short time, of the large data quantity provided by the fleet of 'Family' helicopters (flying up to 100 flight hours per month per aircraft).

A new Flight Conditions Recognition (FCR) algorithm was developed adopting a combination of Machine Learning (M/L) approaches, which are particularly suitable for the analysis of massive data set structures (Big-Data). These data are the time series of the principal flight parameters recorded during the entire life of the helicopter by the HUMS systems fitted on board.

Many advantages are expected from the proper knowledge of the real usage of these helicopter fleets, such as:

- Improvement of flight safety by validation of the design assumptions;
- Reduction of maintenance costs and direct operative costs by reducing unscheduled maintenance and unexpected failures;
- Definition of improved maintenance manuals, with replacement times and inspection intervals tailored to the customer actual usage.

This task is part of the LHD plan for EPAS 2020-2024 (European Plan for Aviation Safety) on 'ageing of the fleet'.

Helicopter maintenance plans are defined on the basis of expected mission profiles, that may be quite different with respect to the actual scenario in which the helicopters will operate. The definition of an improved maintenance plan can be achieved through a periodical validation of the initial usage hypothesis, that can confirm or suggest proper amendments.

A research programme has been developed, in cooperation with two Departments of the Polytechnic of Milan (Department of Mechanical Engineering and Department of Electronics, Information and Bioengineering), with the purpose of developing an advanced analytics software tool set, capable to provide an automatic, reliable and efficient analysis of the time histories of the principal usage parameters recorded on board during flight operations. The final objective is to recognise the rotorcraft flight conditions and their occurrence or duration, to monitor the actual Fatigue Usage Spectrum.

Figure 9 explains the logic of the approach; Flight Conditions Recognition (FCR) is performed on-ground, at the end of the flight.

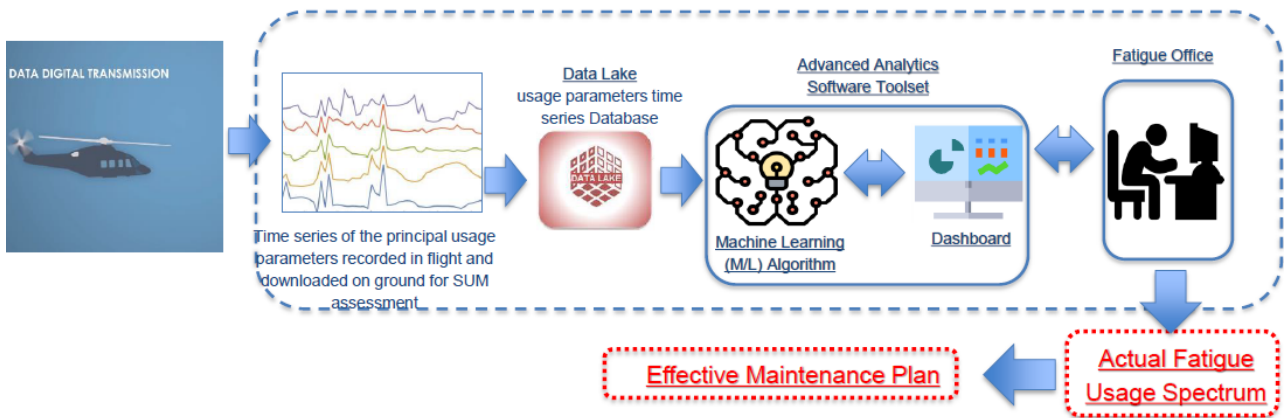


Fig. 9 – Logic of the Flight Conditions Recognition analysis software.

The major challenge of the activity is related to manoeuvre recognition, because of the inherent differences in duration and loading factor that can be ascribed to piloting techniques and to the environment. An additional issue related to manoeuvres is their combination, which may occur in practice when two manoeuvres are executed contemporarily instead of being executed in sequence, like e.g. a rolling pull out or a bank turn associated with a gentle descent or climb.

The data set for training the system by machine learning is made by labelled samples carried out by prototypes and cannot cover all combinations. The issue was solved by extracting statistical features, analysing the time histories by means of ‘sliding windows’ and a supervisor algorithm able to choose the best option.

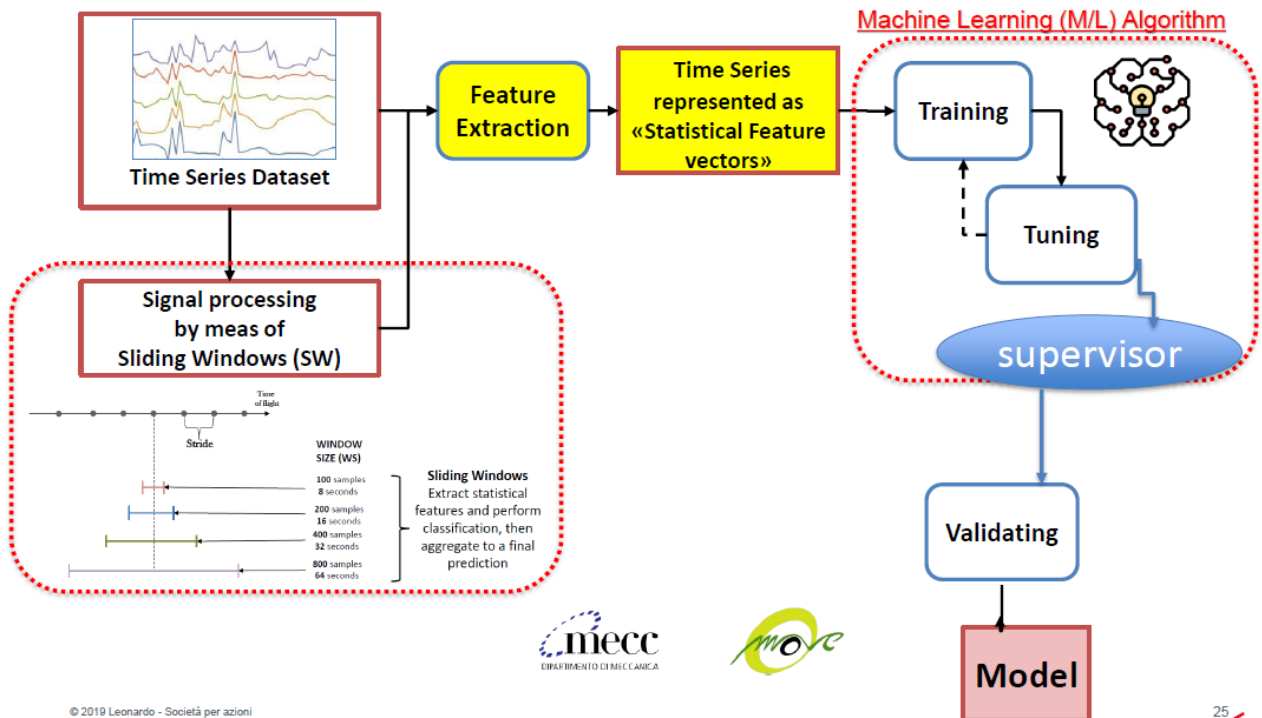


Fig. 10 – Machine Learning (M/L) Algorithm – from Time Histories to Statistical Features for Training phase.

The Dashboard permits to visualize the results of the M/L Algorithm in terms of classified manoeuvres in both a detailed (Flight Explorer) and an aggregated (Helicopter Explorer) way.

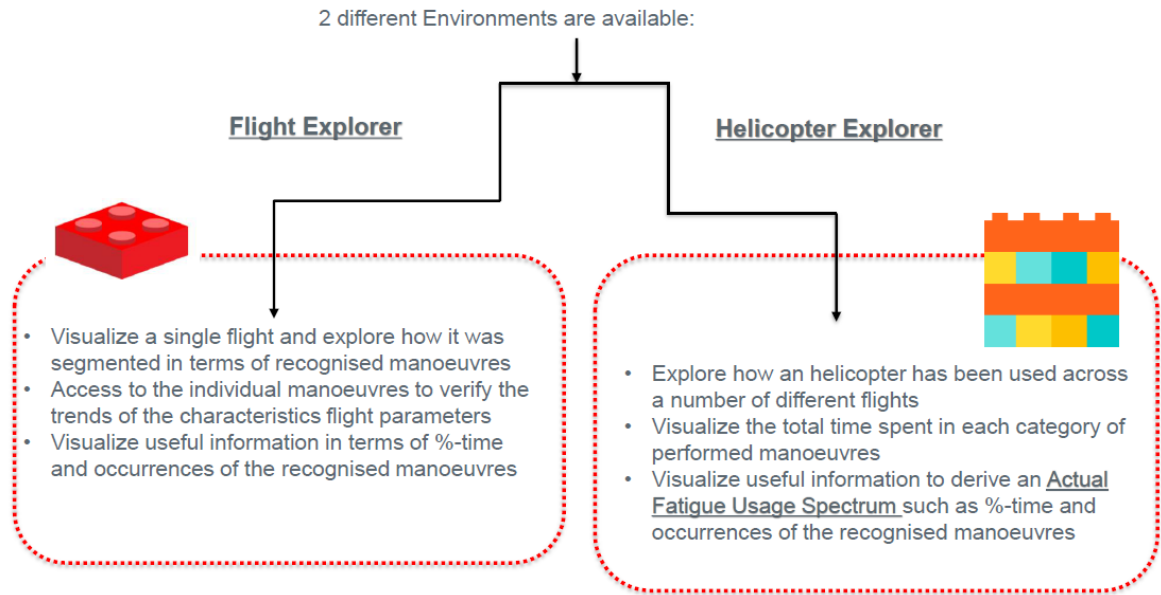


Fig. 11 – Dashboard – Front End interface.

### 2.5 – C-27J Program (Leonardo Aircraft Division)

Information has already been given in previous National Review editions about the C-27J monitoring activity, performed through a specifically developed I.A.T.P. (Individual Aircraft Tracking Program) software, that runs on ground; its aim is to monitor the fatigue life of each aircraft based on the actual mission profiles and load spectra determined by means of the direct recording of in-flight parameters. The I.A.T.P. software compares the aircraft in-service life usage with the design life usage. This allows to plan and manage the fleet usage and the inspection tasks keeping into consideration both the economy and the safety points of view.

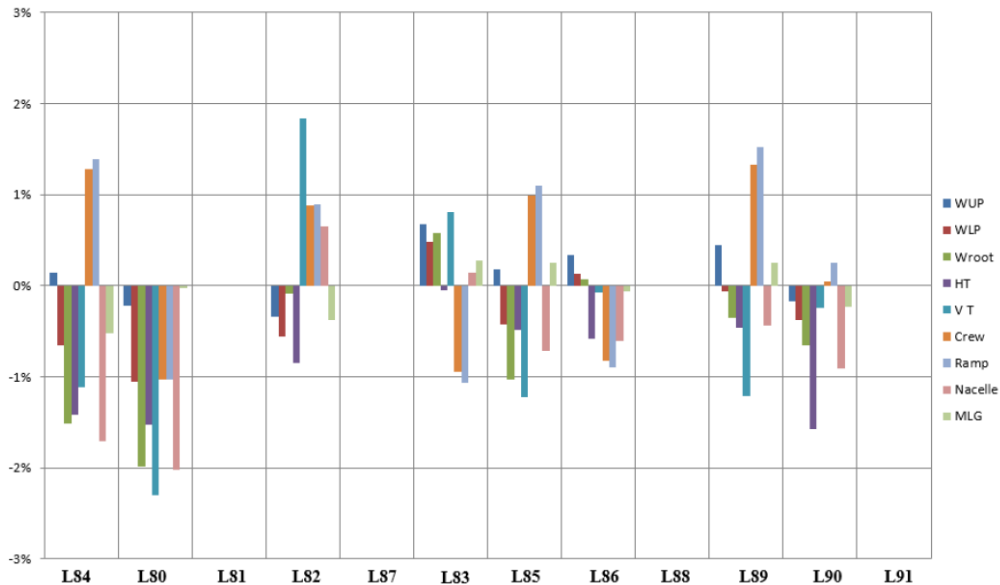


Fig. 12 - LSI percentage variation in the monitored locations, for some aircraft, over the last period.

The software monitors the main representative locations of structural items through the calculation of LSI (Load Severity Index), which is the ratio between the In-Service Life Damage and the Design Life Damage. The Design Life Damage is the fatigue damage calculated under theoretical mission profiles and mixing, which were applied during the full scale fatigue testing. In conclusion, the LSI measures the different severity among in-service and design usage.

Fig. 12 shows, for a number of individual airplanes, the trend of LSI variations in the last period of observation: the fleet fatigue behaviour of the last period is very close to previous one, within a variation of  $\pm 2\%$ . Almost all the LSI are

close to 1.0, except for items sensitive to pressure loads (crew and ramp doors) and to engine loads (nacelles). The fleet typically performs flights of a duration shorter than design and at a higher altitude than design mission profiles.

### 3. METALS

#### 3.1 - Fatigue behaviour of notched and un-notched materials

##### 3.1.1 – Unique Materials for Advanced Aerospace Applications – UMA3 (University of Bologna)

The University of Bologna – Forlì Campus is participating to an aerospace-oriented European project funded within the framework of Horizon 2020: the UMA3 (Unique Materials for Advanced Aerospace Applications) project. The overall aim of the project is to build a value chain consisting of research institutions that are involved in studies on powder metallurgy processes, additive manufacturing, surface technology and fully 3D investigations.

Within the UMA3 project, the goal of the University of Bologna unit is to investigate the use of powder metallurgy and additive manufacturing technologies to provide new solutions for the aerospace industry. In particular, the objective is to study the mechanical behaviour of light alloys components, made by powder metallurgy and additive manufacturing. To this aim, the following steps are under investigation:

- Production of high-performance Al-alloys specimens manufactured by powder metallurgy;
- Mechanical testing of powder metallurgical samples and comparison of their properties with those of samples manufactured by external producers;
- Production of high-performance Al-alloys specimens by additive manufacturing;
- Comparison of the mechanical properties of powder metallurgical and additive manufactured samples.

The expected outcome of this work is to contribute to the characterisation of the microstructural and mechanical properties of components produced by metal powders, which is a fundamental step towards their application alongside with components produced by conventional techniques.

##### 3.1.2 - REACH regulation implementation (Leonardo Aircraft Division)

In the last National Review, information was given about an experimental program, in progress at Leonardo Aircraft Division, for the assessment of the influence of protective treatments, compliant with the current international environmental regulation (**REACH** – **R**egistration, **E**valuation, **A**uthorization and **R**estriction of **C**hemicals), on the fatigue behaviour of the most common metallic alloys. The most well-known case is the elimination of hexavalent chromium, that in the past was used in typical metal surface protection processes; other conversion coating processes are being evaluated.

Specimen ID	Surface Condition	Test Objective
01-PRT	No CCC	S-N basic curve
01-HXV	Hexavalent coating	S-N curve for Hexavalent chemical conversion coating effect
01-SOC	Trivalent Conversion coating Socomore Line	S-N curve for Trivalent chemical conversion coating effect
01-SUR	Trivalent Conversion coating Surtec Line	S-N curve for Trivalent chemical conversion coating effect
02-PRT	No CCC	S-N basic curve
02-HXV	Hexavalent coating	S-N curve for Hexavalent chemical conversion coating effect
02- SOC	Trivalent Conversion coating Socomore Line	S-N curve for Trivalent chemical conversion coating effect
02- SUR	Trivalent Conversion coating Surtec Line	S-N curve for Trivalent chemical conversion coating effect

Legend	
01	2024 T3
02	7075 T6
PRT	Pristine Condition
SUR	Trivalent Conversion Coating type 1
SOC	Trivalent Conversion Coating type 2
HXV	Hexavalent Conversion Coating

Table I – Test matrix for the assessment of the influence on fatigue life of corrosion inhibiting treatments.

A number of fatigue tests have been planned on the most used aluminium alloys, 2024-T3 and 7075-T6; the test matrix is reported in Table I. Each family of specimens will be tested at different stress levels with the aim to have test durations between  $10^4$  and  $3 \cdot 10^6$  cycles.

The fatigue tests are still in progress, but some results can be observed in Fig. 13, where the typical behaviour obtained for AA 2000 series is shown. The same trend of results has been observed for AA 7000 series.

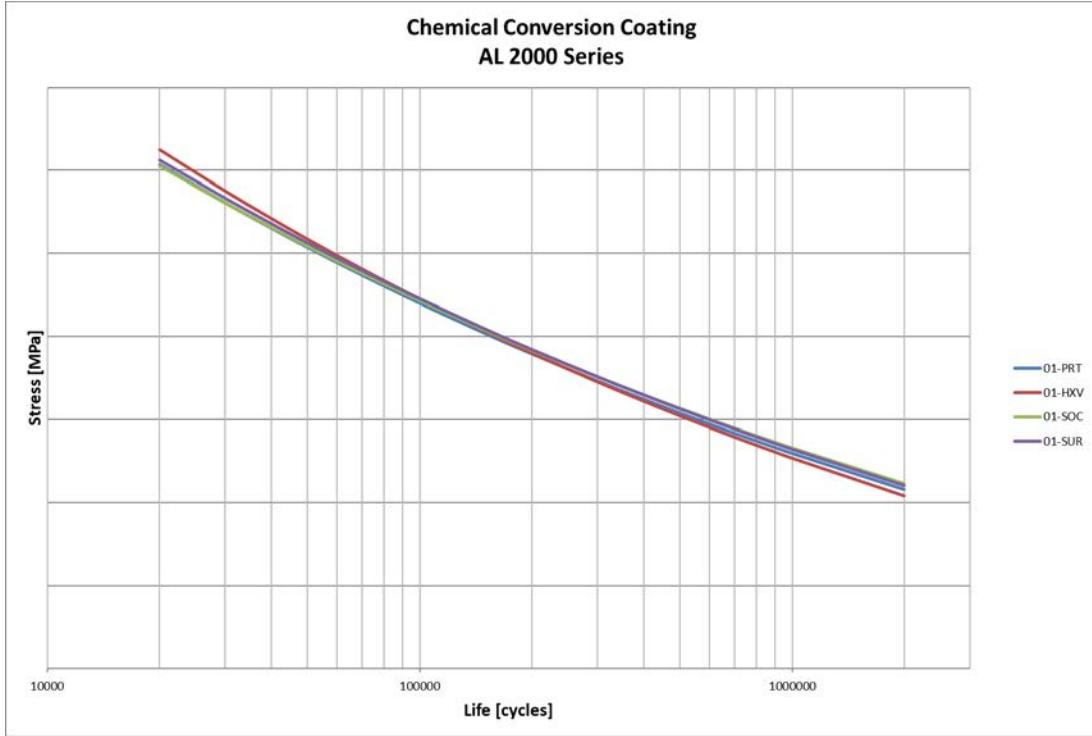


Fig. 13 - Comparison between different protection treatments effects on 2024-T3 fatigue behaviour.

The obtained results show, in all the cases, that the ratio of fatigue allowable between Hexavalent Conversion process and the new ones (SOC and SUR) is always equal or higher than 1.0. So, it can be concluded that the new processes of Chemical Conversion Coating, currently used in Leonardo Company, do not adversely affect the fatigue characteristics of the most common Aluminium series.

Another important protection process for which a substitution is searched is the chromium plating of steel alloys: a thermal spray coating process is under evaluation as an alternative. More details will be given at the end of the evaluation program.

### 3.1.3 – One-up drilling process (Leonardo Aircraft Division)

One-Up Assembly (OUA) is a term that applies to joints that are specifically exempted by engineering authority (data set or drawing), or by the applicable specification(s), from the requirement to clean and/or deburr holes prior to fastener installation.

Leonardo AD planned a test campaign to evaluate the fatigue knock-down factors for one-up drilled hybrid joints (aluminium-composite) containing aluminium elements. Three kinds of joints, in terms of load transfer, have been tested; among them there is also the open hole geometry that represents the no load transfer joint. For each of the above mentioned geometries, specimens with deburred and non-deburred holes have been manufactured. The following table II shows an example of the burr height ranges, in which specimens have been grouped.

Group A [μm]	Group B [μm]	Group C [μm]	Group D [μm]
110 - 129	139 - 150	156 - 170	188 - 206

Table II – Subdivision of specimens according to the range of burr height.

Engineering evaluation of the results is still in progress, but it seems that all the knock-down factors are very close to each other.

**3.1.4 – Fatigue analysis code (Leonardo Aircraft Division)**

Fatigue Analyses, in particular for Damage Tolerance evaluation, are based upon Flight-By-Flight Time Histories. The usage of a Flight-By-Flight Time History permits, due to a more detailed and rich information about the usage, to optimize the structural design of a component from the fatigue point of view but, on the other side, requires the evaluation of the stress associated to each manoeuvre in the Flight-By-Flight spectrum.

The M345 Flight-By-Flight time history, which simulates 500 FH, contains more than 4500 manoeuvres. Forty percent of these manoeuvres are associated with a short time history. In order to perform the fatigue analysis, it is necessary to evaluate  $4500 \times 1.4 = 6300$  stresses for each fatigue location. In order to reduce the analysis effort, a software has been developed applicable both to M345 and to M346.

The software is based upon the idea that the stress in the analysed location is linearly related to a main internal action component. The reference stress acting at the lower main spar cap at wing root section is related to the wing bending moment ( $M_b$ ) through the following equation:

$$S = \frac{M_b}{I} d \quad \text{and hence:} \quad \frac{S}{M_b} = \frac{d}{I}$$

This relation clearly shows that the relation between the reference stress in the section and the bending moment only depends on geometric quantities, which are constant once the structure is defined.

There are locations in which the stress is related to one or more main internal action component (i.e. stress in the wing lower skin may be related to both wing bending and torsion). Also in this case it is possible to define, according to the principle of superposition, the following equation:

$$S = M_b K_b + M_t K_t \quad \text{where } K_b \text{ and } K_t \text{ are appropriate constants.}$$

This may be generalized according to the following equation

$$S = \{K_i\}\{L_i\}^T$$

where the matrix  $L_i$  contains appropriate load conditions.

The evaluation of the coefficient matrix  $K_i$  may be achieved through:

- A static stress analysis with a representative set of load cases
- The use of the Ordinary Least Square methods

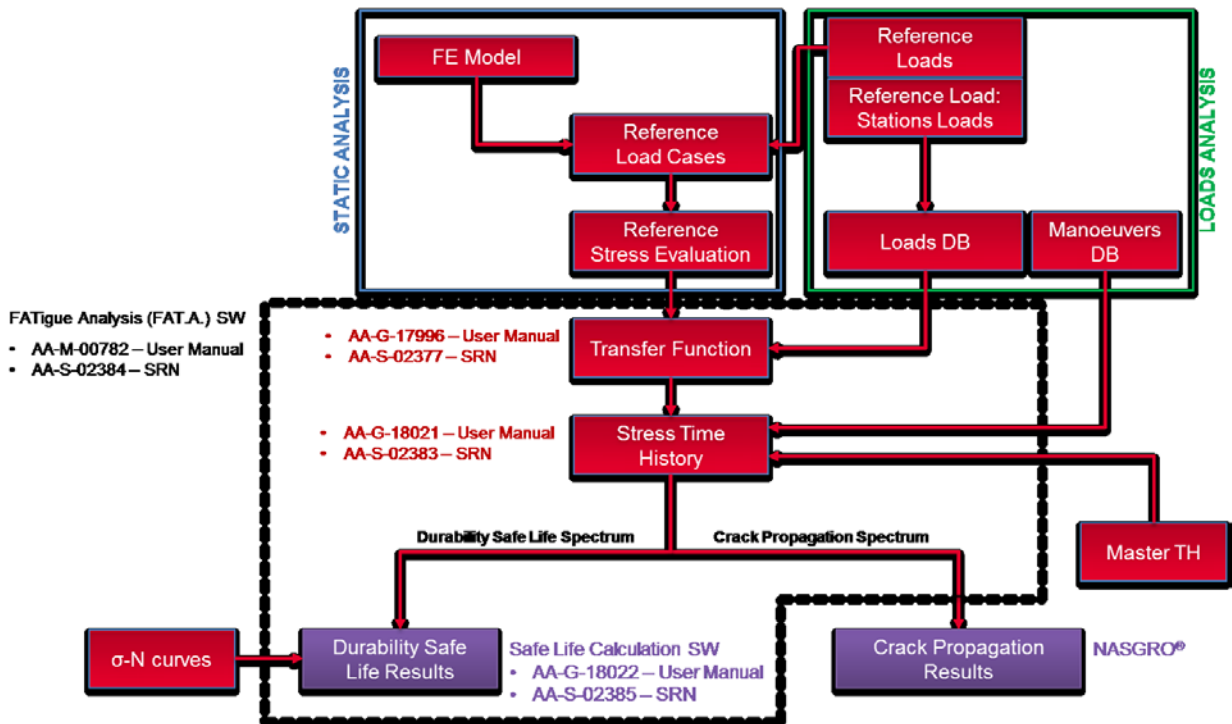


Fig. 14 – Flow chart of the Fatigue Analysis Code (FAT.A.)

The coefficients  $K_i$  are used, in conjunction with the aeromechanical and load simulation software, to evaluate the stress on the fatigue location for every instant of the whole Flight-by-Flight Time History. Therefore, more than 6300 stresses are evaluated starting from representative detailed analysis, that leads to an important time reduction. Once the Stress time history is evaluated, the analysis goes on according to typical fatigue and damage tolerance methodologies.

### 3.2 – Crack propagation and fracture mechanics

#### 3.2.1 – Ti-6Al-4V Investment Casting HIP BSTOA Crack Propagation test data analysis (Leonardo HD)

Crack propagation tests were carried out with the aim of establishing the  $da/dN-\Delta K$  curves in Ti-6Al-4V investment casting HIP BSTOA, in the range  $10^{-8}$ – $10^{-3}$  mm/cycles, for 4 load ratios. The activity was performed in a collaboration with the Polytechnic of Milan – Department of Mechanical Engineering. The activity was performed using SE(B) specimens, designed as per ASTM E399-17.

The tests were carried out in agreement with ASTM E647-15e1 procedure, which means:

- compression pre-cracking at predefined load ratio;
- pre-cracking at the same load ratio of the actual test;
- $\Delta K$ -decreasing method was followed for the near threshold tests;
- specimens were instrumented with 2 crack gauges to measure the crack growth rate;
- the specimens were statically broken at the end of the tests to check the crack front shapes and the crack curvature correction was applied according to ASTM recommendations.

The near threshold behaviour has been investigated with 5 tests per each load ratio, instead of the 2 tests standard procedure, normally followed by LHD.

A statistical analysis of the scatter near threshold,  $\Delta K$  at about  $10^{-7}$  mm/cycle ( $\sim \Delta K_{th}$ ), confirmed that the difference in the scatter assessment between 2 tests and 5 tests is very low and so the standard LHD procedure based on the use of 2 specimens is reliable if tests are carried out according to ASTM E647-15e1 methodology. Table III shows the differences between the  $\Delta K_{th}$  evaluated with 5 and 2 tests.

R	$\frac{\Delta K_{th-5t} - \Delta K_{th-2t}}{\Delta K_{th-5t}}$
-1	1.11%
0.1	9.05%
0.4	4.94%
0.7	-1.83%

Table III – Differences of scatter in the  $\Delta K_{th}$  between 2 and 5 tests repetitions

In addition, a non-dimensional statistical analysis of all the  $\sim \Delta K_{th}$  results was carried out with a Gaussian law and confirmed a consistent value of scatter,  $CV=8\%$ , typically found for this material in safe life and flaw tolerance safe life tests.

#### 3.2.2 - Fatigue crack propagation of 3-D defects (Univ. Pisa)

A research activity is in progress at the Department of Civil and Industrial Engineering – Aerospace Section of the University of Pisa for the study of a comprehensive strategy for capturing fatigue crack growth in complex three-dimensional problems. Corner cracks have been taken into considerations, and two load cases have been examined: one corresponds to an open-hole specimen and the other corresponds to a pin-loaded hole. Experimental data have been generated using 2024-T351 specimens in the course of previous activities, already described in former editions of the National Review.

An adaptive re-meshing technique, based on parametric Python scripts, has been developed to produce regular, structured meshes at different stages of the propagation. Linear FE analyses and the J-integral method are used for the computation of the nominal Stress Intensity Factor (SIF) distribution along the crack front. An engineering methodology, based on elastic-plastic analyses, is implemented for dealing with LFM limitations near free surfaces,

where extensive plastic zones are present. Elastic-plastic analyses are also used for computing the variation along the crack front of the state-of-stress, quantified by the constraint factor, whose value greatly influences the Plasticity-Induced Crack Closure (PICC). Local values of the constraint factor are evaluated and fed to the Newman's model [1] for a local evaluation of the opening stress. No predetermined crack shape is assumed in this analysis (Fig. 15): the shape of the crack is the sole result of the theoretical model and its numerical implementation. Finally, material anisotropy is accounted for by adopting two slightly different FCGR curves.

Fig. 16 shows a comparison with experimental results for the open hole specimen and shows that an accurate, yet computationally heavy, evaluation of all the physical and numerical “parameters” associated with fatigue propagation can produce a good prediction of the corner crack propagation. The proposed approach has the merits that no predetermined crack shape is enforced; a precise and local calculation, along the crack front, of the driving and retarding forces – nominal SIF range and PICC, respectively – can yield accurate results, while preserving the physical significance of all the model’s parameters.

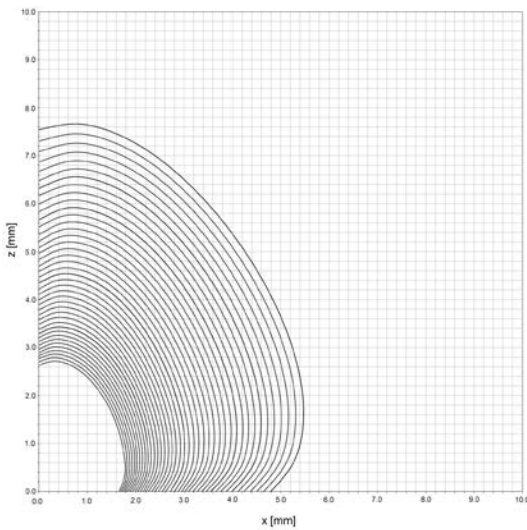


Fig. 15: Crack shape evolution.

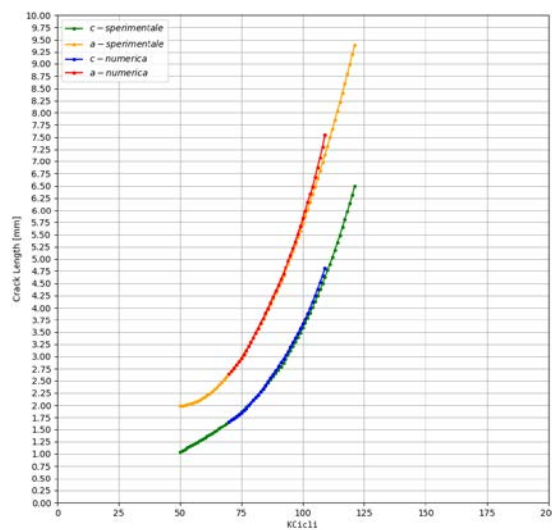


Fig. 16: Comparison between numerical and experimental results.

### 3.3 - Corrosion and fatigue

#### 3.3.1 – Corrosion Effects Assessment on Fatigue Behaviour of Al 7475-T7351 (Leonardo Helicopter Division)

The typical corrosion cases for helicopters are pre-corrosion due to the manufacturing process, like etching for surface treatment or bonding, or in service corrosion, due to improper coupling of materials or to degradation or damage of protections. The number of corroded items increases with the size of the fleet, the exposure to aggressive environment and the ageing of the aircrafts. For these reasons, this task is part of the LHD plan for EPAS 2020-2024 (European Plan for Aviation Safety) on ‘ageing of the fleet’.

Corrosion effects on fatigue strength may be correlated to the material data base of micro cracks from Kitagawa plots, in order to support any life assessment for reuse or continued usage, to validate the life prediction and the inspection interval in service and to address any crack growth from corrosion pit or corrosion increase. LHD has developed a comprehensive data base of Kitagawa diagrams for the structural materials used in helicopters and this validation would extend their usage to corrosion defects.

A research project is currently on-going with the Polytechnic of Milan (Departments of Mechanical and Chemical Engineering) in order to verify the equivalence of the flaw tolerance behaviour of defects, with the same transversal dimension (expressed in terms of  $\sqrt{Area}$ ), produced by electro-erosion and by different corrosion procedures:

- **Artificial and accelerated corrosion:**
  - A1) Electrochemical attack
  - A2) Salt spray exposition
  
- **Natural corrosion:**
  - N1) Urban environment exposition
  - N2) Marine environment exposition

The comparison is for threshold of non-propagation of small cracks like defects, used to build the Kitagawa diagram and its application domain. The scope is therefore the evaluation of the threshold of non-propagation of small defects. Aluminium Alloy 7475-T7351 has been selected as first material to be investigated, being typically used for helicopter dynamic parts.

The first group of tests to be performed, also to obtain a reference datum for comparison with subsequent results, was carried out on EDM specimens with R=0.1. The Stair-case (Hodge-Rosenblatt) method was used to define the endurance limit, and the test was considered a “Run-Out” if it survived  $10^7$  fatigue cycles.

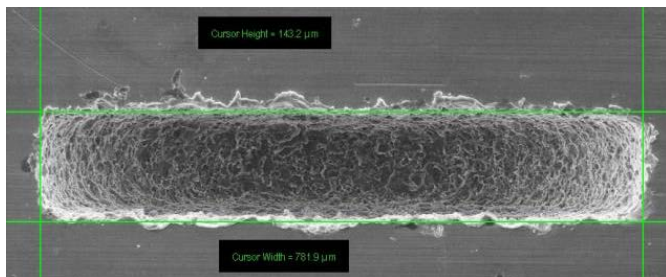


Fig. 17 - EDM defect measured by SEM

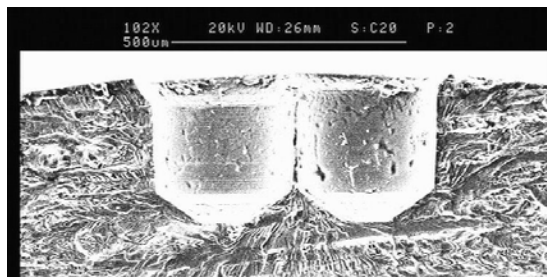


Fig. 18 - Micro-notched specimen

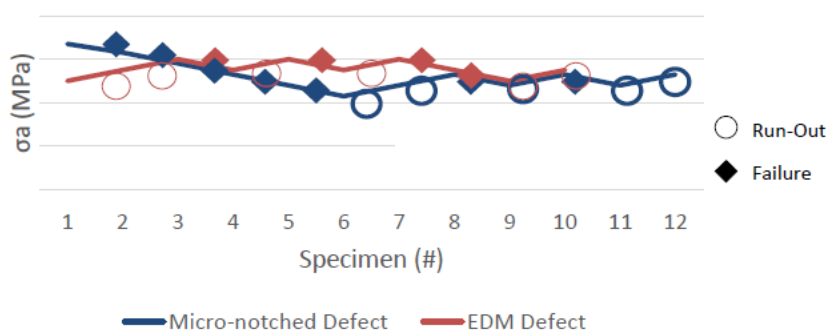


Fig. 19 - Comparison of fatigue limit for the specimens containing the two types of defects.

#### Artificial processes

##### A1) Electrochemical Attack – Galvano-static procedure

25 specimens have been subjected to a Galvano-static procedure designed “*ad hoc*” for promoting a localized corrosion pit with geometric characteristics similar those of EDM specimens, with a target  $\sqrt{\text{Area}}$  of 0.445 mm.

Procedure duration time: 10 hr 8 min (*from Faraday's Law*)

The specimens have been examined to characterize the shape and depth of the defect, in order to make comparisons with the other types of damages.

##### A2) Salt Spray exposition

25 specimens have been subjected to Salt Spray exposition in agreement with *ASTM B117 – Standard Practice for Operating Salt Spray*.

Procedure duration time: 1 month

##### N1) Urban environment exposition

15 specimens are exposed to an urban environment (Milan) and are monitored each month.

Procedure estimated duration time: 1 year

##### N2) Marine environment exposition

15 specimens are exposed to a marine environment (Bonassola, SP) and are monitored each month.

Procedure estimated duration time: 1 year

### Fatigue Tests on Corroded Specimens –Tests Results

A subset of 12 specimens, electrochemically corroded through the Galvano-static procedure, has been selected for similarity with the EDM specimens defect, adopting the criterion of minimizing the discrepancy of the mean  $\sqrt{Area}$ . The selected 12 corroded specimens have been subjected to the Stair-case sequences to identify the fatigue limit at  $10^7$  cycles and stress ratio  $R=0.1$ . The results are shown in Fig. 20 (in green), together with those already presented in Fig. 19, i.e. those belonging to EDM (Fig. 17) and micro-notch specimens (Fig. 18); a similarity in results can be observed.

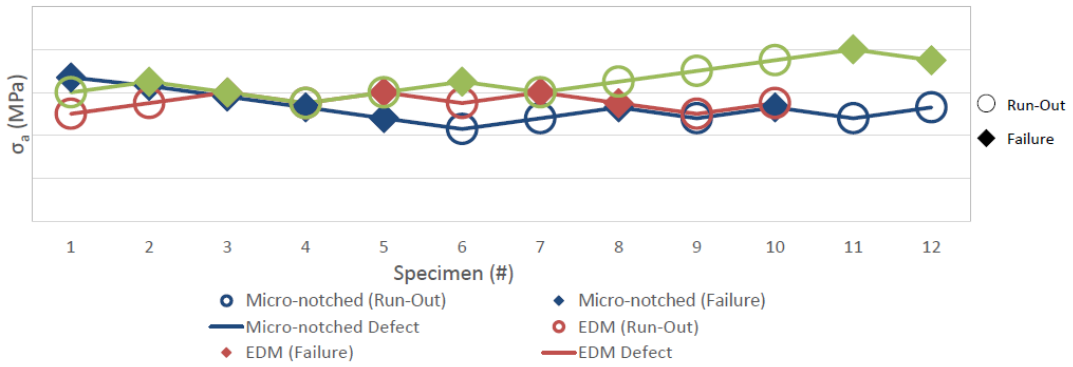


Fig. 20 – Comparison of endurance limit test results for different types of defects in 7475-T7351.

### 3.4 – Structural Health Monitoring

#### 3.4.1 – Structural Health Monitoring – Acoustic Emissions (Univ. Bologna)

Structural Health Monitoring (SHM) aims at shifting aircraft maintenance from a time-based to a condition-based approach. Within all the SHM techniques, Acoustic Emission (AE) allows for the monitoring of large areas by analysing Lamb Waves propagating in plate like structures. A Time Reversal (TR) methodology is proposed with the aim of reconstructing an original and unaltered signal from an AE event. Although the TR method has been applied in Narrow-Band (NwB) signal reconstruction, it fails when a Broad-Band (BdB) signal, such as a real AE event, is present. Therefore, a novel methodology based on the use of a Frequencies Compensation Transfer Function (FCTF), which is capable of reconstructing both NwB and real BdB signals, has been developed at the University of Bologna – Forlì Campus. The study was carried out experimentally using several sensor layouts and materials (see a sketch in Fig. 21) with two different AE sources: (i) a Numerically Built Broadband (NBB) signal, (ii) a Pencil Lead Break (PLB). The results were validated numerically using Abaqus/CAE with the implementation of absorbing boundaries to minimize edge reflections.

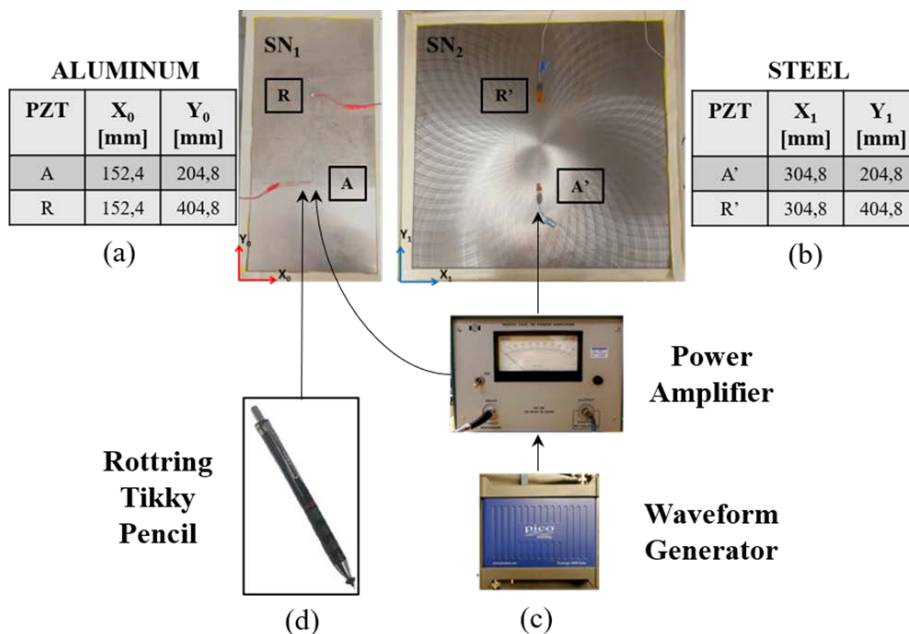


Fig. 21 - Experimental sensor networks SN1 (Al) and SN2 (Steel).

The methodology used in the study carried out at the University of Bologna – Forlì Campus has been divided into three phases for clarity.

- I. Analytical description of the TR method for BdB signals: The application of a FCTF to the TR method is described mathematically, thereby developing a strategy to reconstruct a generic BdB signal.
- II. Experimental Application: The FCTF TR process is applied experimentally to reconstruct NBB and PLB signals on a thin aluminium sheet (1.6 mm thick), followed by the reconstruction of NBB signals on a thick steel plate (13 mm thick).
- III. Computational Verification: Validation of the analytical technique was performed through the development of a numerical model (Fig. 22 shows some details of the area modelled, on the right) using Abaqus/CAE. The TR process was applied to NBB and PLB signals.

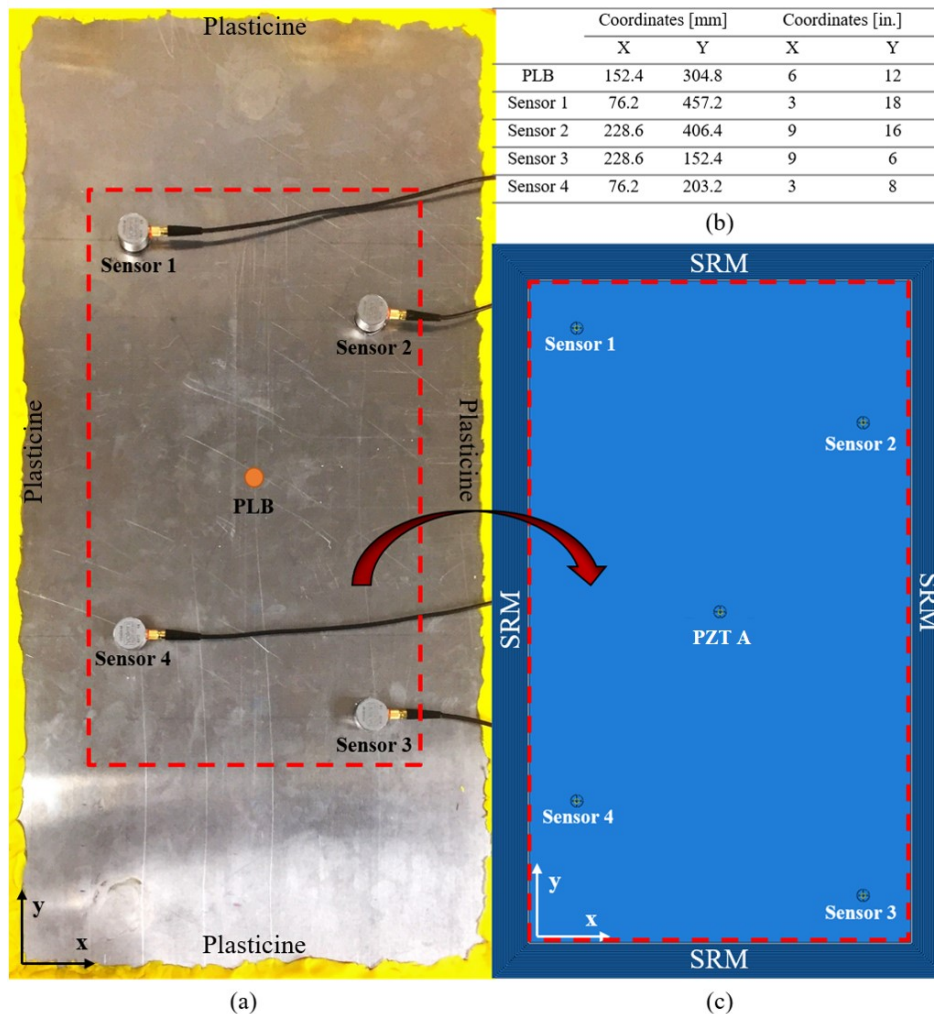


Figure 22 – Physical experimental set-up and configuration used for the numerical analysis.

Further details can be found in references [1-3].

## 4. COMPOSITES AND FIBER METAL LAMINATES

### 4.1 – Investigation on Disbond Arrest Features in adhesive joints (Univ. Bologna)

An investigation is in progress at the University of Bologna – Forlì Campus on Disbond Arrest Features (DAF), considered an attracting option to improve the fracture behaviour of adhesively bonded joints. The term Disbond Arrest Feature denotes any design feature which can be used to retard or stop the crack growth. For adhesively bonded joints this usually means stopping the crack growth in the adhesive layer, i.e. disbonding.

The work investigates fatigue crack growth in bonded GLARE specimens with a bolted disbond arrest feature. To this end, Cracked Lap Shear (CLS) specimens have been used, modified by installing an Hi-Lok in the centre, as shown

in Fig. 23. The CLS configuration allows to reproduce a mixed-mode ratio which is comparable to that found in real aeronautical components. All the tests have been conducted under fatigue tensile-tensile loading. The crack length was measured visually by a camera aimed at the specimen side and using an algorithm based on digital image correlation measurements. A 3D finite element model of the bolted CLS specimen was developed to compute the strain energy release rate (SERR).

The results of the fatigue tests show that the Hi-Lok has a retarding effect on disbond growth, as can be seen in Fig. 24. The tests evidenced the formation of secondary cracks in the GLARE adherents, which forced the stop of the test before complete disbonding could occur. The numerical results are shown in Fig. 25: the SERR distribution around the DAF changes significantly, with a reduction of mode I component and an increase of mode II component.



Fig. 23 - Bolted cracked lap shear specimens. Both flat and flush head Hi-Loks have been employed.

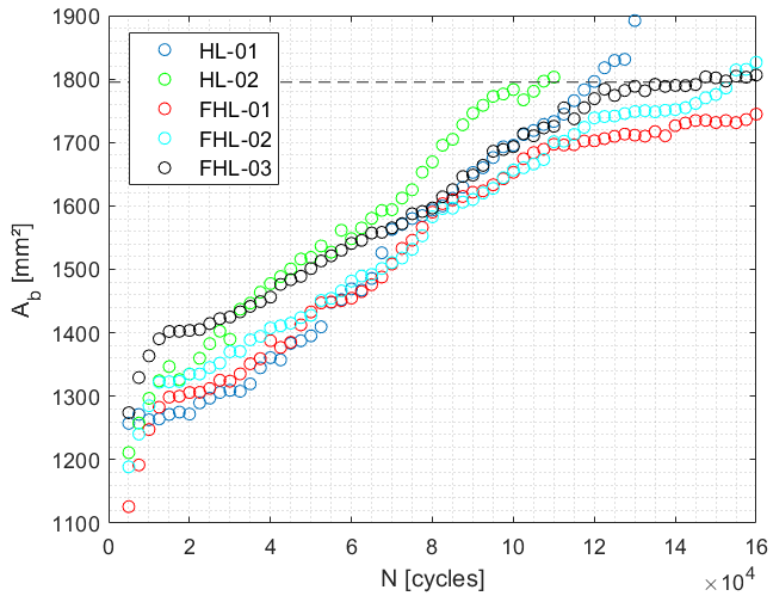


Fig. 24 - Fatigue crack growth measured by the digital image correlation algorithm. The horizontal dashed line represents the position of the Hi-Lok.

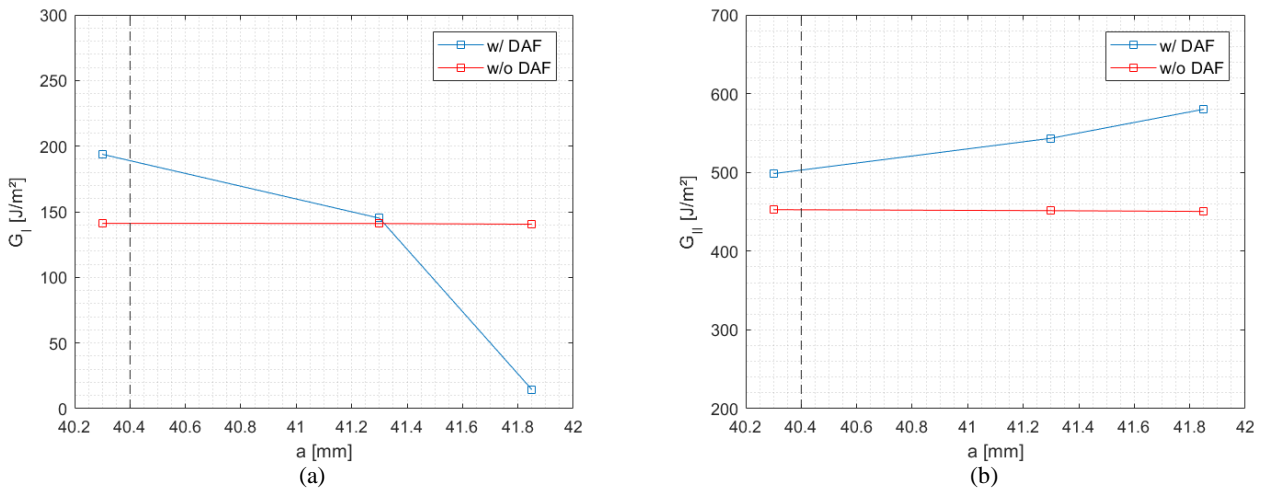


Fig. 25 - Strain Energy release rate assessed by the finite element model. The two components of the SERR are shown: (a) Mode I, (b) Mode II.

Further research efforts aim at the development of a prediction model of disbond growth in adhesive joints with bolted disbond arrest features. More details can be found in references [4-5].

#### 4.2 – Effects of thermal residual stresses on the structural integrity of hybrid and composite elements (Milan Polytechnic)

A research is in progress at Milan Polytechnic, Department of Aerospace Science and Technology (DAER), to develop approaches to predict damage modes, failures, and residual strength of composite structures by taking into account the presence of thermal residual stress. Such thermal residual stresses develop in the manufacturing as a consequence of the difference in the coefficients of thermal expansion (CTE) of the different components or lay-ups: a clear understanding of the curing process is needed. An experimental program has been carried out at DAER of Milan Polytechnic, using specimens specifically designed and manufactured: two different hybrid metal-composite laminates and a pure composite.

In the first phase of this activity, the build-up of thermal residual stresses inside composite and hybrid elements during manufacturing is studied. The proposed lay-up design of the specimens is shown in Figure 26, where two lay-ups are described: Symmetrically Cracked (SC) and Asymmetrically Cracked (AC). The SC specimen had been designed to control the development of thermal residual stress while the AC was designed to exaggerate this effect. Three samples of AC and SC have been produced, and two of each batch were sensorized by FBG sensors carried by optical fibre with the aim of assessing the strain evolution during the manufacturing, focusing on the cooling phase (Figure 27).

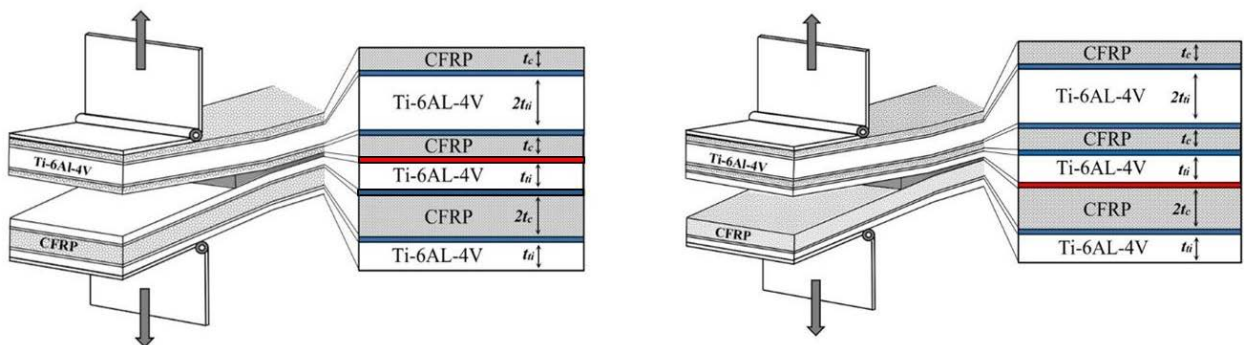


Fig. 26 – Sketches of the lay-ups of hybrid DCB specimens (Symmetrically Cracked on the left, Asymmetrically Cracked on the right; the red line indicates the delamination position).

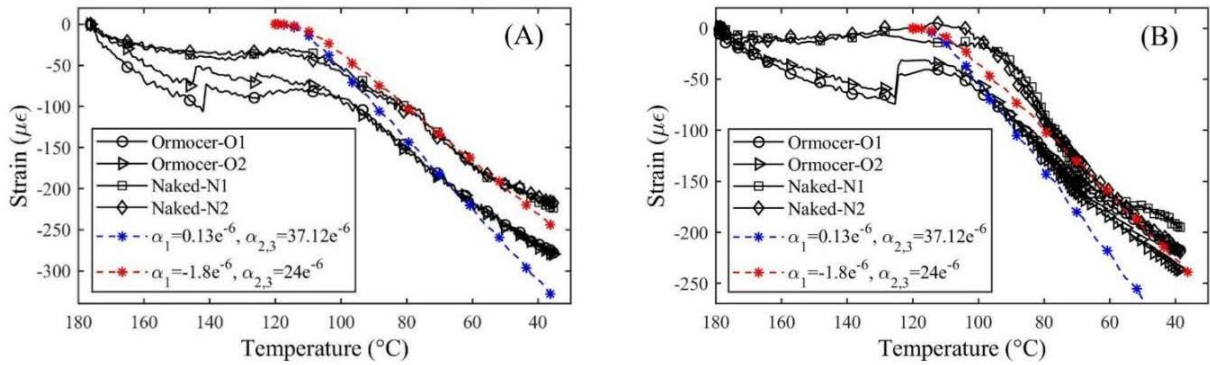


Fig. 27 – Experimental and numerical strain evolution during cooling.

A numerical modelling of the cooling process has been performed using Simulia/Abaqus software. To simplify the analysis, in the cooling process the phases where the material shows viscoelastic behaviour in the range from 180 $^{\circ}\text{C}$  to 120 $^{\circ}\text{C}$  have been omitted, so considering only the temperature range from 120 $^{\circ}\text{C}$  to 20 $^{\circ}\text{C}$ . Fig. 27 presents the experimental and numerical results of strain evolution during the cooling phase of SC and AC specimens. The value of the CTE was calibrated in such a way that the remaining strain at the end of the cooling phase meets the experimental results.

Adhesive layer in numerical modelling is represented using finite thickness elements with embedded cohesive zone model, developed at DAER Department [6]. With the help of this numerical modelling technique, two numerical analyses were performed: a single-step analysis without consideration of cooling analysis and a multistep analysis with cooling simulation. By comparing these two analyses, the amount of thermal residual stress and their effect on the fracture behaviour is assessed.

Double Cantilever Beam (DCB) tests for mode I fracture toughness were performed; the embedded sensors measured the strain evolution inside the material during the tests. The comparisons of experimental and numerical results of force versus displacement in DCB tests are shown in Figures 28: the SC specimens is on the left (Fig. 28-A) and the AC specimen on the right, in Fig. 28-B. It must be observed that the numerical results obtained with and without the preliminary cooling analysis are superimposed and are in good agreement with the experimental results, in both loading and unloading phases. Also the results of FBG sensors, not shown here or brevity, have the same trend. Numerical results are identical for both analysis procedures and capture very well the experimental behaviour. These results indicate that the thermal residual stresses do not affect the damage evolution in the SC specimen, as expected.

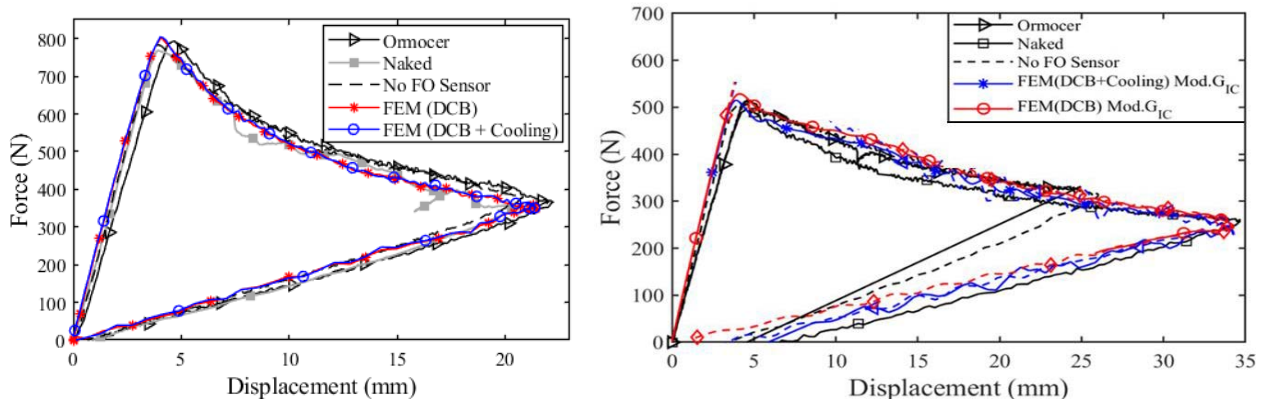


Fig. 28 - Experimental and numerical results of DCB tests for A) SC and B) AC

However, at the initiation of damage in AC, a slight difference between the two types of numerical analyses can be observed, particularly more evident in the unloading phase. The numerical simulation with consideration of cooling analysis was able to capture the remaining displacement at the end of unloading (in SC specimens, this remaining displacement did not exist). The effect of thermal residual stress is significantly higher in the strain evolution measured by FBG sensors during the crack propagation.

The research includes also another study, again relevant to the effect of thermal residual stress on the damage behaviour, but applied to curved laminates with different lay-ups. The interlaminar and intralaminar failure modes in the curved composite specimen is a complex phenomenon, and the investigation aims at studying experimentally and numerically the complex interlaminar damage scenarios in thick composite specimens with multidirectional stacking sequences. A novel nonlinear modelling approach has been evaluated. For this purpose, two lay-ups of [0]<sub>48</sub> (Zero) and

$[0_2/90_2]_{6s}$  (Crossply) have been studied. Three specimens of each lamination were manufactured with unidirectional Hexcel AS4/8552 pre-pregs.

Figs. 29 and 30 show the final shape of the specimen after manufacturing in comparison with the lower mould. The spring-in is significantly higher in the Crossply laminate than in the Zero laminate, which indicates the existence of residual thermal stress in the Crossply laminate. Linear Cooling analysis was performed in the temperature range of 180°C to 20°C. The analysis results indicate that the Crossply specimen is experiencing a high amount of in-plane stress after the cooling while the stress state in the Zero specimen is almost negligible. Therefore, the cooling analysis of the Crossply must be considered as a preloading condition.

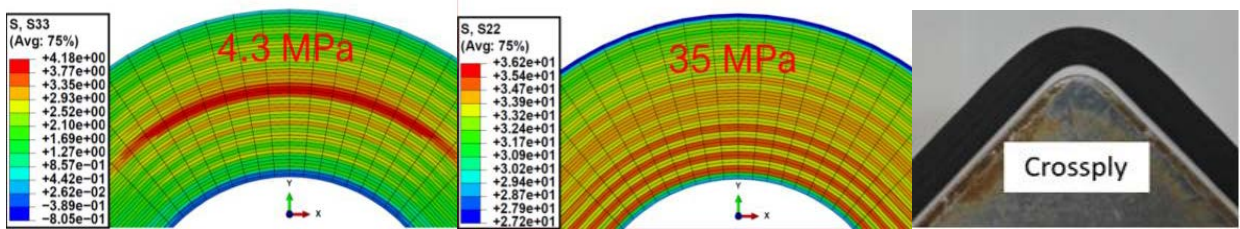


Fig. 29 - Comparison of Spring-In and in-plane and out-of-plane stress contour in Crossply specimen.

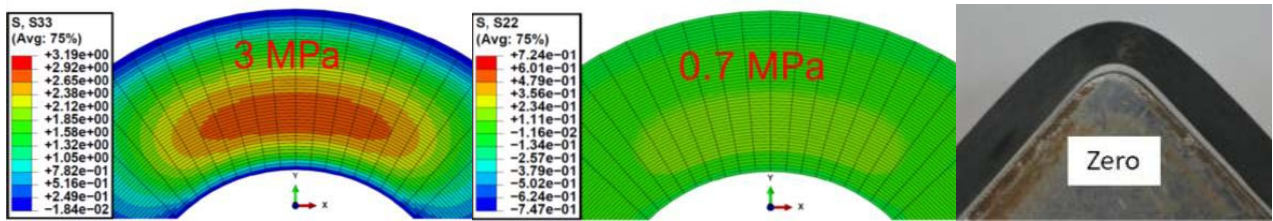


Fig. 30 - Comparison of Spring-In and in-plane and out-of-plane stress contour in Zero specimen.

In the Zero layup (Fig. 31), the first loading cycle caused a catastrophic failure that reduced the specimen stiffness close to zero. The failure mechanism is pure delamination. In all three specimens, one main crack, positioned at one-third of the thickness from the inner side of the curvature, dominated the damage scenario; other cracks, distributed all over the thickness, have been arrested in the curved zone.

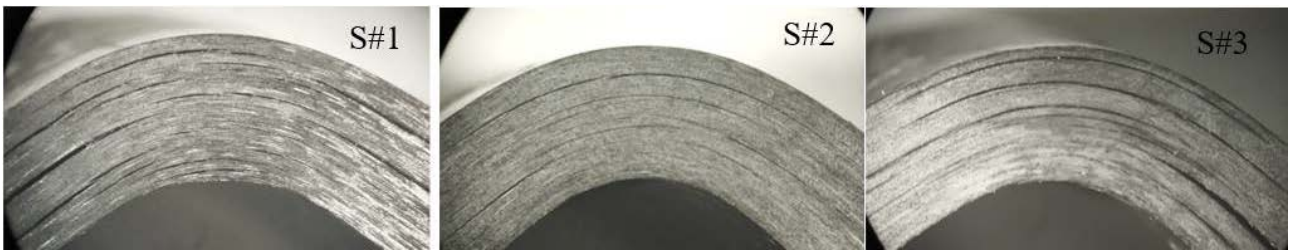


Fig. 31 - Interlaminar crack evolution for Zero specimens,  $[0]_{48}$ .

Figure 32 illustrates the failure modes of the Cross-Ply specimens, that are significantly different from those of the Zero specimens. The specimens did not lose all their loading capability in the first failure, so a second loading cycle was applied to these specimens. It is apparent from the results that failure started with matrix cracking, then these cracks propagated to cause the delamination between the 0 and 90 oriented layers. The first crack is located in one-third of the thickness from the inner side of curvature, the same interface of the Zero lay-up specimens.

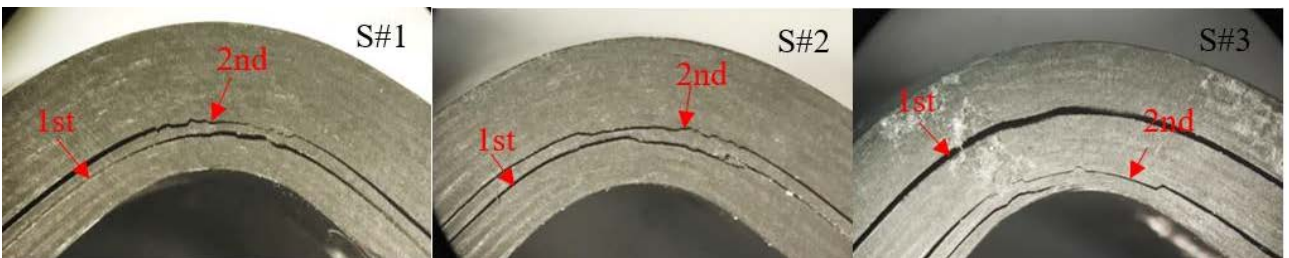


Fig. 32 - Interlaminar crack evolution for Crossply specimens,  $[0_2/90_2]_{6s}$ .

For the simulation of damage behaviour of both lay-ups, the new non-linear modelling technique developed in [7] has been used. This modelling technique avoids the need for very high penalty stiffness levels for conventional cohesive elements, which, in an explicit time integration scheme, will directly affect the stable time step and leads to very high computational costs. To overcome this problem, the non-linear analysis presents a novel modelling technique based on the cohesive damage law to model the interlaminar damage evolution, keeping into consideration the different roles played by the in-plane and the out-of-plane stress components. In this modelling technique, the basic hybrid modelling has been modified and improved to a bi-phasic approach to increase the accuracy of simulating the different phases of composite.

The results of the simulations are in good agreement with the experimental observations. In the case of the Zero specimen, delamination was identified as the main failure mode and the position of the main crack was estimated with accuracy. In the more complex case of the Crossply specimen, the numerical results show that intralaminar damage develops first, leading subsequently to interlaminar damage development; the interaction between different forms of damage is captured with appreciable accuracy.

### 4.3 - Structural Health Monitoring by means of Optical Fibres (Uni. Bologna)

The use of optical fiber sensors (OFS) is diffused in the Structural Health Monitoring (SHM) community for their ability to detect many different physical quantities, its robustness against electromagnetic disturbances, its light weight and embedding possibilities. The last point has been widely investigated for different types of materials, but only recently researchers considered the possibility to embed optical fibres in 3D printed structures. Additive Manufacturing (AM) offers new opportunities for the manufacturing of structures with complex geometries in a relatively short time. However, new challenges must be considered, including innovative embedding solutions for different types of sensors.

As a first step, current embedding strategies for optical fibre sensors in structures produced with the Fused Deposition Modelling (FDM) technique have been analysed in a research program performed at the University of Bologna – Forlì Campus. A novel methodology to embed OFS (outlined in Fig. 33) has been tested through the production of specimens at three different filling densities and six different loads. The experimental results (the set-up is shown in Fig. 34), where both distributed OFS and strain gauges were used, were also compared with the data obtained from a numerical model developed in Abaqus/CAE in which the filling pattern of the specimens was accurately reproduced, highlighting both agreements and discrepancies with respect to the expected data. Fig. 35 shows the comparison between measured and numerically assessed strains. More details can be found in references [8-10].

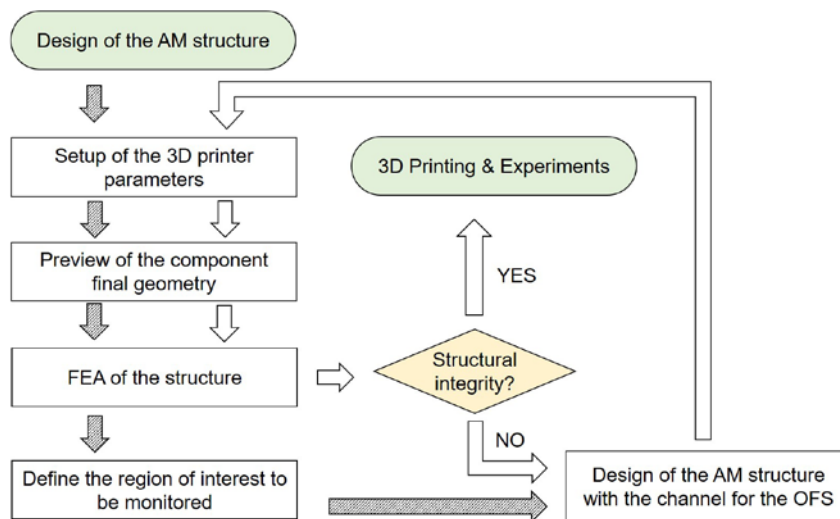


Fig. 33 - Flowchart for the embedding methodology for the OFS inside the AM structure

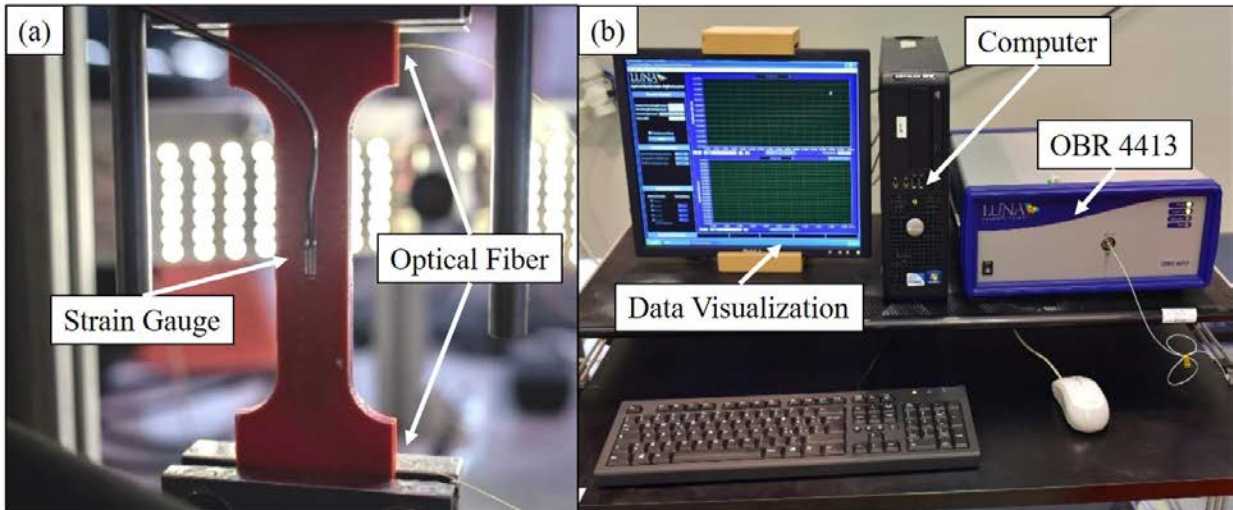


Fig. 34 - Specimen during the tensile test (a), and data acquisition system with the OBR 4413 (b).

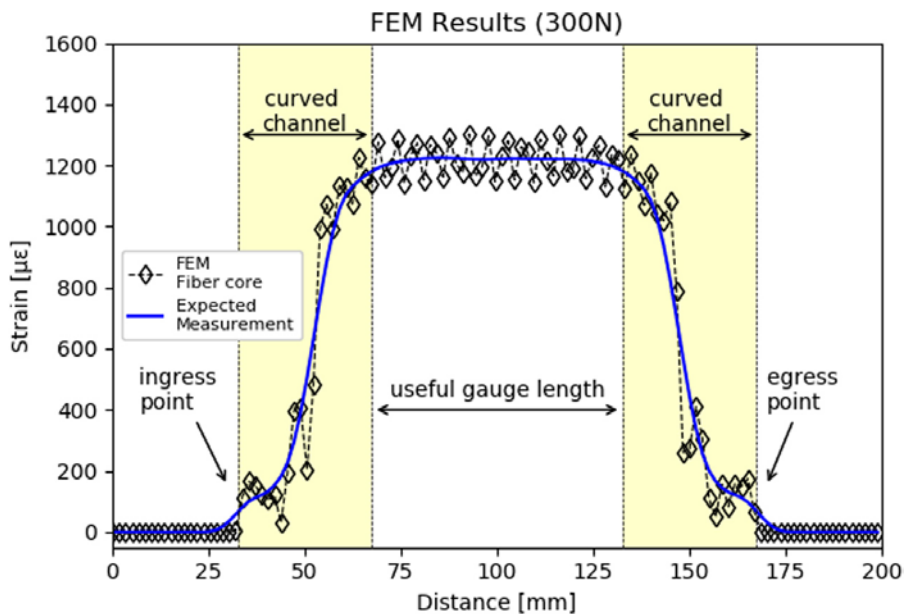


Fig. 35 - Numerical results at 300 N and 40% filling density.

#### 4.4 - Obsolescence of Composite Materials of PSEs (Leonardo HD)

The composite material of the AW189 Main Rotor Blade Spar was changed due to supplier changes in production lines. Certification of the New Blades was carried out by the Building Block approach proving that the new production is at least equivalent to the previous standard.

Full Scale Fatigue Testing on the most critical Main Rotor blade specimen (see figure 36) is at the top of the pyramid, while Structural Elements testing provides scatter factors for both static and fatigue analysis. Point design were used for evaluation of details not addressed by Full Scale Test; coupon tests were used for the data base of lamina properties (RTD, RTW, HTW) and constitute the basis of the test pyramid.

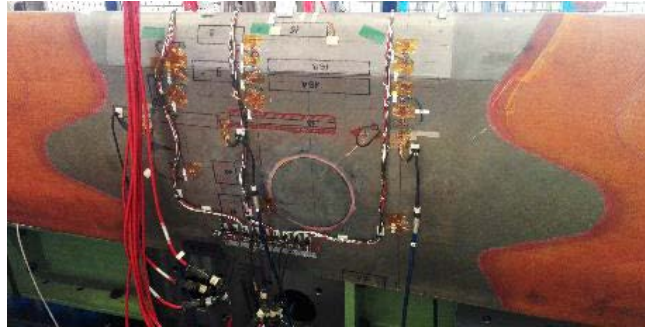


Fig. 36 – Full scale fatigue testing of an AW189 Main Rotor blade section specimen.

## 5. NDI METHODS

### 5.1 - Probability of Detection for Visual Inspection (Leonardo Helicopter Division)

14 CFR§29.571 Amdt. 29-55 (2 December 2011) requires, for each Principal Structural Element (PSE), a **threat assessment** which includes the determination of the probable locations, types, and **sizes** of damage to be used in the fatigue tolerance evaluation.

For Transmission Metallic Components not exposed to damage in service, Leonardo Helicopter Division proposed to consider the minimum size defect that can be **reliably detected** by the relevant Detailed Visual Inspection (DVI), as the maximum size defect that can remain undetected in the PSE (Barely Detectable Flaw, BDF).

Fig. 37 shows an example of the DVI toolbox:



Fig. 37 – Content of the Detailed Visual Inspection toolbox.

AC 29.571B (2 December 2011) suggests that, if the current capability of a specific inspection method is in question, then the assessment should include the determination of the **Probability of Detection (POD)** as a function of damage size. Leonardo Helicopter Division therefore proposed to conduct a **Point Estimate Probability of Detection survey** for inspecting 0.30 mm long - 0.15 mm deep - 0.10 mm wide, “half-penny” shaped artificial defects made in carburized steel mechanical components. Artificial defects were inflicted to the test specimens using Electro-Discharge Machining (EDM).

Point Estimate is based on defect Length ( $L = 0.30$  mm). The Depth is determined as half of the Length, to obtain the typical semi-circular cross section used in the damage tolerance analysis. The Width is determined as the smallest that can be achieved with EDM, and it is consistent with the Width of real case scratches on metallic components.

Examples of scratches are reported in the following figures 38 and 39:

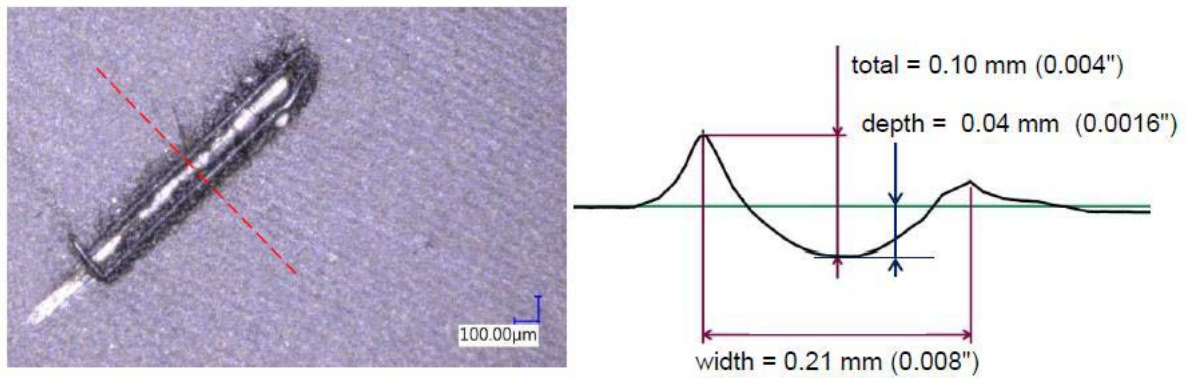


Fig. 38 – Example of defect dimension measurements.

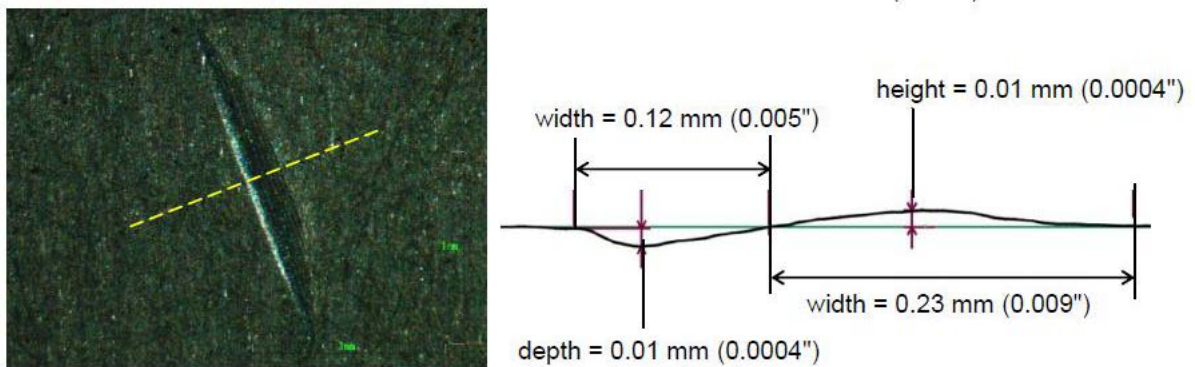


Fig. 39 – Another example of scratch measurements.

Statistical analysis

A reliably detectable flaw has been defined as the flaw that can be detected with a probability of detection of 90% at a confidence level of 95% (POD<sub>90-95</sub>).

The binomial distribution of probability (appropriate for the Hit/Miss visual inspection data) is used to determine the number of successes (Hits), out of the total number of trials, that provides a 90% probability of success with a 95% lower confidence bound.

$$C_L = \frac{d}{d + (n - d + 1)F_\alpha(f_1, f_2)}$$

$$f_1 = 2(n - d + 1) \quad f_2 = 2d$$

Where:

$C_L$  is the lower confidence interval at (1- $\alpha$ )%;

$F_\alpha(f_1, f_2)$  is the  $\alpha$  percentile of the F-distribution with  $f_1$  and  $f_2$  degree of freedoms.

$n$  is the number of trials (hit/misses)

$d$  is the number of hits.

Number of trials	Number of hits	Number of misses
29	29	0
46	45	1
61	59	2

Experimental activity, on test specimens

A total 29 artificial defects will be inflicted on 10 different gears (actual aircraft components). Test specimens have been selected based on the worst-case surface finishing for defect visibility. The defects are randomly distributed on the test specimens, from a minimum of 0 defects to a maximum of 4.

The following three photographs (fig. 40) show the specimens:



AW139 TR TakeOff Pinion      AW169 Pinion, 2<sup>nd</sup> stage, RH      AW609 Pinion, 2<sup>nd</sup> stage, RH

Fig. 40 – Examples of the specimens used for the statistical analysis of the PoD assessment.

The test specimens will be inspected by 3 different inspectors qualified to conduct the DVI for Transmission Metallic Components, using the same tools and procedures adopted during manufacturing. Each inspector's findings are considered independent from each other. All three inspectors are required to find all 29 defects to ensure inspector variability is accounted for.

Findings will be recorded in the Inspection Report Cards. The inspectors will be unaware of the scope of the inspection, number and position of the artificial defects. Natural defects present in the test specimen, if detected, will not be considered for the scope of the survey. The result of the survey is to be considered positive if all the 29 artificial defects are detected.

## 6. AIRCRAFT FATIGUE SUBSTANTIATION

### 6.1 - Damage tolerance of AW249 attack helicopter (Leonardo Helicopter Division)

AW129 is the attack helicopter in service for the Italian Army. It has been qualified in the 90's; fatigue tolerance are evaluated with safe life approaches, in fully compliance with the applicable rules of the time. Historically, the A129 was the first attack helicopter developed in Europe.

The AW249 is the new generation attack helicopter currently under development. The qualification will account for the latest safety standards for fatigue, with a full damage tolerance qualification, in line with AC29 civil rules.

#### Flaw Tolerance Data And Analysis

*Threat assessment* evaluates potential damages, as a result of both manufacturing and service operations.

*Stress Analysis* identifies critical locations and stress levels.

*Material characteristics* are evaluated by tests on coupon with defects to derive:

- $\Delta\sigma_{TH}$  Threshold stress below which a crack will not propagate from the defect
- Pristine versus Flaw Reduction Factor  $K_{P/F}$  (effect of the defect on the fatigue strength)

#### Damage Tolerance – Metal Parts

Dynamic parts are evaluated with flaw tolerance approaches verifying that the stress due to flight loads are below the propagation threshold (no-growth approach). Crack propagation analyses are generally applied to structural parts only. They are performed using NASGRO® and proprietary crack propagation data, which are generated internally, on a routine basis, using standard specimens and procedures.

### Flaw Tolerance – Composite Parts

The component parts are qualified according to the building block approach, performing:

- Tests on coupons, performed to derive:
  - SN Curve Shape
  - Coefficient of Variability (CV)
  - Room Temperature Wet degradation (RTW)
- Tests on full parts, including defects and impacts
  - At the end of each fatigue test, the residual strength up to Ultimate Load is demonstrated

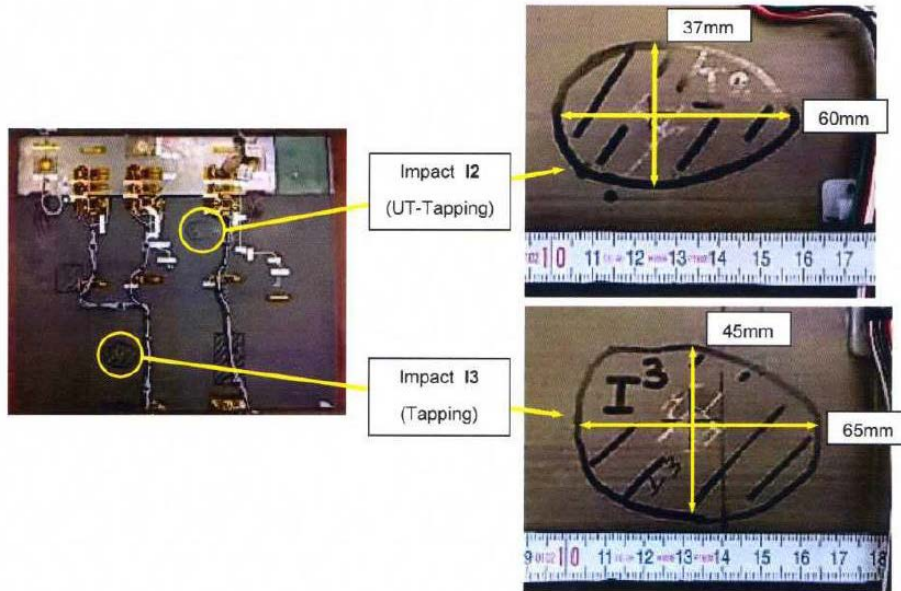


Fig. 41 – Damaged full scale parts subjected to damage tolerance tests.

Some images relevant to impact damaged full parts are reported in Fig. 41.

### 6.2 - AW189 / AW139 / AW169 helicopter family (Leonardo Helicopter Division)

In the last two years, a number of improvements have been introduced on the three helicopters of the family (AW169 is the smallest and AW189 is the largest). Some of them are often the consequence of the end of the certification test, with a clearance extended to a longer life for replacement; also mandatory inspections of fatigue critical parts were updated accordingly. In the following, some examples of the fatigue life reassessment for AW169 and AW189 components are given. Improved fatigue evaluations were carried out for these extended performances and the new limitations were reported in Helicopter Maintenance Manual as appropriate (for AW169 and AW189):

#### a) AW169

Some customers reported high occurrences of rescue hoist usage, significantly higher than assumptions for Type Certificate. Therefore, a comprehensive fatigue reassessment due to the change of loading spectrum was required for these users, addressing both the increased occurrence of rescue hoist loading cycles and the higher occurrence in hovering and manoeuvres in hovering.

Reduction of maintenance costs was obtained also as a consequence of the life extension of the Tail Rotor Hub and of the Life Extension of Main Cabin assy, up to 20000 FH or 80000 Landings.

#### b) AW189

For the AW189 helicopter, an extension of the Flight Envelope of the GE engine configuration up to 15000ft was obtained and another engine (SAFRAN) with increased available power is under evaluation (Full Envelope to be certified in 2021).

Reduction of maintenance costs was obtained also as a consequence of the life extension of Tail Rotor blade and removal of calendar life limitation: a Full Scale fatigue test was performed on a conditioned Tail Rotor blade specimen for environmental ageing.

## 7. REFERENCES

- [1] Pascoe, J.A., Zavatta, N., Troiani, E., Alderliesten, R.C., “The effect of bond-line thickness on fatigue crack growth rate in adhesively bonded joints”, *Engineering Fracture Mechanics*, 2020, 229, 106959.
- [2] Zavatta, N., Troiani, E., “A numerical approach to the disbonding mechanism of adhesive joints”, *Lecture Notes in Mechanical Engineering*, 2020, pp. 360–371.
- [3] Falcetelli, F., Venturini, N., Romero, M.B., ...Pant, S., Troiani, E. “Broadband signal reconstruction for SHM: An experimental and numerical time reversal methodology”, *Journal of Intelligent Material Systems and Structures*, 2021, 32(10), pp. 1043–1058.
- [4] Venturini, N., Martinez, M., Troiani, E., Barroso-Romero, M., Falcetelli, F., “Experimental broadband signal reconstruction for plate-like structures”, *Proceedings of 30th International Conference on Adaptive Structures and Technologies, ICAST 2019*, 2019, pp. 123–124.
- [5] Falcetelli, F., Romero, M.B., Pant, S., Troiani, E., Martinez, M., “Modelling of pencil-lead break acoustic emission sources using the time reversal technique”, *9th European Workshop on Structural Health Monitoring, EWSHM 2018*, 2018.
- [6] Airoidi A, Sala G, Bettini P, Baldi A. An efficient approach for modeling interlaminar damage in composite laminates with explicit finite element codes. *Journal of Reinforced Plastics and Composites*. 2013;32(15):1075-91.
- [7] Airoidi A, Mirani C, Principito L. A bi-phasic modelling approach for interlaminar and intralaminar damage in the matrix of composite laminates. *Composite Structures*. 2020;234:111747.
- [8] Falcetelli, F., Di Sante, R., Troiani, E. “Strategies for Embedding Optical Fiber Sensors in Additive Manufacturing Structures”, *Lecture Notes in Civil Engineering*, 2021, 128, pp. 362–371.
- [9] Bastianini, F., Bochenski, P., Di Sante, R., ...Rossi, L., Bolognini, G., “Strain Transfer Estimation for Complex Surface-Bonded Optical Fibers in Distributed Sensing Applications”, *Proceedings of 2020 Italian Conference on Optics and Photonics, ICOP 2020*, 2020, 9300327.
- [10] Falcetelli, F., Rossi, L., Di Sante, R., Bolognini, G., “Strain transfer in surface-bonded optical fiber sensors”, *Sensors (Switzerland)*, 2020, 20(11), 3100.